buildings

MDPI

Article

Comparison of Fragility Sets to Assess the Effectiveness of Retrofit Interventions on Masonry Buildings in Italy

Veronica Follador [1,*], Pietro Carpanese [1], Marco Donà [1], Sara Alfano [2], Serena Cattari [2], Sergio Lagomarsino [2] and Francesca da Porto [1]

[1] Department of Geosciences, University of Padova, Via Gradenigo 6, 35131 Padova, Italy; pietro.carpanese@unipd.it (P.C.); marco.dona.1@unipd.it (M.D.); francesca.daporto@unipd.it (F.d.P.)
[2] Department of Civil, Chemical and Environmental Engineering, University of Genova, Via Montallegro 1, 16145 Genova, Italy; sara.alfano@edu.unige.it (S.A.); serena.cattari@unige.it (S.C.); sergio.lagomarsino@unige.it (S.L.)
* Correspondence: veronica.follador@unipd.it

Abstract: Seismic events that have occurred in Italy in recent decades have shown the significant vulnerability of the Italian building stock. In particular, residential masonry buildings have suffered serious damage, highlighting the need to plan effective mitigation strategies as soon as possible. In this context, this study aims to evaluate the effectiveness of possible retrofit interventions for masonry buildings. Fragility curves of macro-classes of residential masonry buildings have been developed in both as-built and retrofitted conditions within the DPC-ReLUIS agreement (Department of Civil Protection—Network of University Laboratories for Earthquake Engineering). In particular, three sets of fragility curves, developed by the University of Padova (UniPD) and the University of Genova (UniGEa and UniGEb) are discussed and compared herein. The three models show similar estimates of the expected structural improvements for the examined retrofit interventions when applied to the building macro-classes, although some differences, due to the different analysis approaches, can be observed.

Keywords: seismic risk; vulnerability model; fragility curves; retrofit interventions; mitigation strategies; masonry residential buildings

Citation: Follador, V.; Carpanese, P.; Donà, M.; Alfano, S.; Cattari, S.; Lagomarsino, S.; da Porto, F. Comparison of Fragility Sets to Assess the Effectiveness of Retrofit Interventions on Masonry Buildings in Italy. *Buildings* **2023**, *13*, 2937. https://doi.org/10.3390/buildings13122937

Academic Editor: Maria Teresa De Risi

Received: 17 August 2023
Revised: 4 November 2023
Accepted: 19 November 2023
Published: 24 November 2023

1. Introduction

Italy is frequently struck by seismic events, with seismic risk being the cause of the highest losses in terms of human lives and reconstruction costs. Seismic events have indeed led to economic losses of 180 billion euros in the past 50 years [1]. The evaluation of seismic vulnerability, which plays a key role in countries like Italy with a consistent number of historical buildings, is particularly relevant for the assessment of seismic risk [2–4].

To address this challenge, the Italian Department of Civil Protection (DPC) is working in a close relationship with members of the scientific community, such as ReLUIS (Italian Network of the University Laboratories of Seismic and Structural Engineering), to develop reliable fragility models and seismic risk maps of Italy, which are useful for supporting the emergency phase and for identifying effective risk mitigation strategies [5].

In particular, the WP4 MARS project (Seismic damage and Risk MAps of Risk) 2019–2021 had, among its goals, the review, update, and comparison of existing vulnerability models for residential buildings in Italy [6,7] as well as the extension of the risk assessment to other strategic (like school and hospital buildings, see [8]), industrial, and monumental (like churches, see [9]) assets. To produce risk maps, the project relied on the use of fragility curves, which are probabilistic cumulative distributions that link the probability of the occurrence of a certain damage state (DS) to a specific seismic intensity parameter, such as the peak ground acceleration (PGA) [10]. Recent studies supported by the DPC have proposed the development of fragility models associated with macro-classes

of Italian residential buildings, drawn according to the Italian national building census [11]. Such macro-classes are herein named ISTAT types and are defined by a combination of three main parameters, i.e., the structural type, age of construction, and number of storeys. Different methods have been deployed to derive fragility curves, including mechanical models [12,13], empirical approaches [14–16], and empirical–heuristic methodologies [17]. Enhanced probabilistic frameworks have been also developed for the selection and generation of earthquake records [18–20] and for the definition of failure modes and related limit states [21,22] to improve the reliability of fragility analyses. In this context, the Italian scientific community involved in the MARS project not only worked towards the definition of fragility curves for buildings in their as-built state but also considered seismic retrofit interventions to assess the effectiveness of possible mitigation strategies and the corresponding reduction in potential losses. Task 4.6 of the abovementioned WP4 MARS 2019–2021 project focused on the elaboration of vulnerability models for retrofitted buildings and the creation of maps of mitigated risk [23,24]. While experimental and numerical analyses of different retrofit solutions for the various structural typologies (masonry, reinforced concrete, precast concrete, steel, etc.) have been objects of research for a very long time, the scientific community has only begun to address the issue of the impacts of interventions on the fragility of building classes recently. Indeed, the increasing losses caused by seismic events are a testament to the relevance and urgency of providing not only retrofit interventions for single building types but also efficient retrofitting strategies and mitigation plans on a broader scale.

In particular, some recent studies have looked into the efficacy of risk reduction techniques for reinforced concrete (RC) buildings. For example, the work presented in [25] deals with the selection of optimal seismic retrofit solutions for RC buildings, where concrete jacketing, the addition of concrete walls, and the addition of steel braces are the alternatives considered. Other studies have focused on the retrofitting of RC structures that do not conform to modern seismic design requirements using various techniques, among which fibre-reinforced-polymer wrapping of columns and joints, RC and steel jacketing [26], or even the application of external sub-structures, such as the precast bolt-connected steel-plate-reinforced concrete-buckling-restrained brace frame (PBSPC BRBF) [27].

Conversely, although some recent studies have begun to investigate the effects of past interventions in masonry buildings through observational approaches [28,29], there is still a research gap regarding the fragility assessment of masonry buildings with the application of retrofit interventions. This paper aims to fill this gap by presenting the activities carried out within the previously mentioned Task 4.6 of the WP4 MARS 2019–2021 by the three research units of the University of Padova (UniPD, led by F. da Porto) and the University of Genova (UniGEa, supervised by S. Lagomarsino, and UniGEb, coordinated by S. Cattari). The work focused on the definition of fragility curves for macro-classes of unreinforced masonry (URM) buildings, both in their as-built configuration and after applying retrofit interventions.

In this paper, possible retrofit interventions for URM buildings are briefly illustrated, including interventions that increase the wall strength and compactness, interventions that improve wall-to-wall and wall-to-floor connections, and mitigation strategies that increase the horizontal diaphragm stiffness. The abovementioned interventions were simulated individually or combined. In the following sections, a general overview of the three methods is provided, highlighting their similarities and differences. The results in terms of fragility curves are then compared with the as-built fragility curves elaborated by each research unit to estimate the improvement provided by each intervention. The outcomes of fragility curves simulating the retrofitted conditions are also compared with each other to understand how the characteristics of each method influence the mitigated fragility. The purpose of this paper is indeed to evaluate the performances of different retrofit interventions and the possible differences in the results obtained by the three approaches.

2. Selection and Modelling of Retrofit Interventions for Masonry Buildings

Reference literature [30] as well as field observations [4,31] were used to choose the most common retrofit solutions for different macro-classes of residential masonry buildings. The interventions were divided into three categories based on the type of improvement that they are intended to bring: (a) increases in wall strength and compactness (MSN1, MSN2, MSN); (b) improvements in wall-to-wall and wall-to-floor connections to ensure box-like behaviour (TR, CR); and (c) an increase in the horizontal diaphragm stiffness (FLR). The considered interventions can be applied to a masonry building singularly or in combination with each other to enhance their effectiveness. Figure 1 lists the interventions that were chosen for two building categories based on the construction period of the buildings, i.e., buildings designed before 1945 (historical buildings) and buildings designed after 1945 (modern buildings). In particular, the year 1945 was selected as the turning point because of the rapid increase in construction technology that the massive post-war reconstructions triggered in Italy, moving away from the traditional techniques used until then. Each intervention shown in Figure 1 is given a synthetic name and may include different specific intervention techniques based on the type of building on which they are applied, as further explained below.

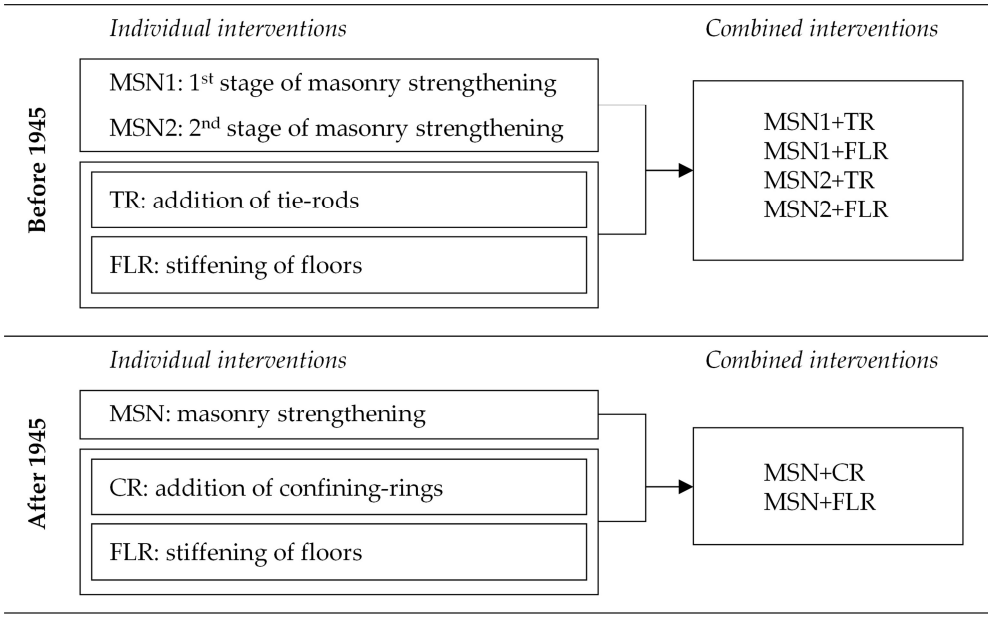

Figure 1. Selected retrofit interventions for different construction periods.

Regarding the interventions on masonry walls, historical buildings are supposed to have two possible stages of application (MSN1, MSN2). The first stage of the masonry intervention (MSN1) considers the application of lighter or local techniques, whereas the second stage (MSN2) suggests the simultaneous application of two or more techniques or the extensive implementation of a heavier one. On the other hand, one-step retrofit interventions are considered for modern buildings (MSN) due to the better as-built quality and condition of the masonry. Concerning historical buildings, the load-bearing structure is usually composed of stone or solid brick masonry. In case of inconsistent random stone masonry, the considered intervention is grout injection, since it is one of the most common and effective ones [32,33]. This technique consists of filling the voids within the wall with natural hydraulic lime-based grouts, which ensure a high level of homogenisation with the existing materials. Conversely, reinforced plaster or FRCM-TRM (Fibre-Reinforced Cementitious Mortar—Textile Reinforced Mortar) interventions are implemented in case of stone ashlars and brick masonry [34–36]. The latter is also considered for strengthening modern buildings composed of solid or hollow brick masonry. This intervention consists of plaster made of fibre meshes coated in inorganic matrices (lime or cement mortar)

applied to the entire surface of the walls. The aforementioned interventions (injections and reinforced/FRCM-TRM plasters) were simulated in combination with bed-joint repointing or reinforced bed-joint repointing (in the case of regularly coursed masonry) and with transversal connection elements (in the case of multi-leaf stone masonry).

When modelling interventions to ensure the box-like behaviour of the building, the main choice has been steel tie-rods (TRs) for historical buildings [37–40] and confining rings (CRs) made from steel bars or bands of FRP/SRG (Fibre-Reinforced Polymers/Steel Reinforced Grout) placed all around the buildings in the case of more modern ones [41]. The former consist of steel bars placed at the roof level connecting parallel opposite walls to prevent out-of-plane mechanisms and to better redistribute in-plane loads. The latter has the same function as the tie-rods but is applied externally, completely surrounding the building in a closed ring. In both cases, the assumption that masonry is sufficiently compact and resistant was made, so that it could be deemed capable of supporting the anchors and the forces that they generate locally.

Lastly, due to the major differences in floor typologies between historical and modern structures, different building construction periods need distinct floor interventions (FLR). To improve the stiffness of the wooden horizontal diaphragms, which are typical in ancient buildings, wooden planking reinforcement with adequate connections to the walls was taken into consideration [42,43]. Wooden planking consists of the addition of single or double wooden planks over the existing ones placed in the orthogonal direction or at 45°. When dealing with modern buildings, poor RC and hollow-tile floors are commonly encountered, so in this case, the simulated intervention consisted of replacing (or inserting) the concrete slab with the addition of adequate connections to the joists and to the walls around the building perimeter.

For a more comprehensive description of the proposed retrofit solutions, reference can be made to [24].

3. Approaches for Deriving Fragility Curves and Implementing Retrofit Interventions

3.1. Methods used for the Derivation of Fragility Curves

Different approaches can be used to derive fragility curves; in particular, three different methods were applied in this work:

- A macroseismic–heuristic method, proposed by the research unit of UniGEa (the University of Genova).
- A simplified mechanical–heuristic method, proposed by the research unit of UniPD (the University of Padova);
- A simplified mechanical method, proposed by the research unit of UniGEb (the University of Genova).

Each method is briefly described below; for further details, please refer to the specific literature listed for each approach.

The macroseismic–heuristic method adopted by UniGEa [17,44] is a method based on the expertise that is implicit on the European Macroseismic Scale (EMS98 scale) [45] but that has recently benefitted from the fitting of the available Italian post-earthquake damage. The method is derived from the EMS98 vulnerability classification and the vulnerability curve concept originally introduced by [44], which assumes a regular increase in the mean damage with the earthquake intensity and is derived with fuzzy assumptions on the binomial damage distribution. More specifically, the method defines the two parameters V (vulnerability index) and Q (ductility index) of the macroseismic vulnerability curve (Equation (1)) by fitting observed damage data in the domain given by the mean damage (μ_D) and the macroseismic intensity (I).

$$\mu_D = 2.5\left[1 + \tanh\left(\frac{I + 6.25V - Q - 10.8}{Q}\right)\right] \quad (1)$$

The vulnerability curve obtained by replacing the fitted V and Q values in Equation (1) is then converted into the corresponding set of fragility curves using the binomial probability distribution and an appropriate PGA (Peak Ground Acceleration)-I correlation rule. In particular, the relationship PGA = $c_1 c_2^{I-5}$ was adopted, where c_1 is associated with the PGA value for I = 5 and c_2 expresses the increasing PGA factor due to an increase of 1 in the macroseismic intensity (c_1 = 0.047 and c_2 =1.7 in this work). Equation (1) implicitly assumes the completion of Damage Probability Matrixes according to the binomial probability distribution. The fitting of observed data made in the μ_D—I domain, which is addressed to define the V and Q values, is particularly efficient, particularly in cases of scarcity or irregularities of the statical samples, as discussed in [46].

The simplified mechanical–heuristic procedure adopted by UniPD [13] is based on the use of Vulnus vb 4.0 software [47,48] developed in previous years by the University of Padova and recently updated. Vulnus analyses load-bearing URM buildings on the basis of their geometry (floor plan and elevation), material properties (tensile and compressive strength and specific weight), and construction details (e.g., the presence of containment elements). In addition, qualitative information is collected based on parameters included in the GNDT level II form [49], such as the masonry quality, floor and roof types, plan, and elevation regularity. The software is based on the calculation of three indices. The first two indices are associated with mechanical resistance and are V_{IP}, which represents the shear resistance of the building, and V_{OP}, which is basically a triggering out-of-plane acceleration that is representative of the building's behaviour and is derived from the critical acceleration of several possible out-of-plane mechanisms (i.e., overturnings, bending and arching mechanisms). The third index V_V is related to qualitative information that is relevant to assess the vulnerability of the building, and it is calculated from the information collected in the GNDT level II form. Through the calculation of these three indices and the adoption of the Fuzzy sets theory, Vulnus produces a fragility curve, which represents a moderate–severe damage state (DS2-3 on a scale from DS1 to DS5), as a function of the PGA. Complete fragility sets from DS1 to DS5 are then obtained by calibrating the macroseismic fragility model of Lagomarsino and Cattari [50]. In particular, the fragility curve produced by Vulnus and the fragility curves related to the DS2-3 of the macroseismic model (from class A to class F) were compared. The optimal solution between the minimisation of the absolute error between the curves, according to the least squares method, and the minimisation of the relative error, expressed as the difference in the positive and negative areas between the curves was then used to combine the fragility sets (DS1–DS5) of the macroseismic vulnerability classes and to generate a fragility set related to the Vulnus fragility curve.

Lastly, the DBV-Masonry (Displacement-Based Vulnerability) mechanical method used by UniGEb [50,51] produces fragility curves of URM buildings starting from analytical definitions of the main parameters (acceleration at yielding, period, and displacement capacities) that characterise the building's capacity curve through the explicit dependence on a limited number of mechanical (i.e., shear strength and shear modulus of masonry, specific weight of masonry, drift limit values of piers, seismic floor loads) and geometrical (i.e., inter-storey height, ratio of resistant walls over the gross in-plan area) factors; moreover, assumptions about the modal shape are required. The pure analytical computation of the capacity curve is firstly conducted under the assumption of perfect box-like behaviour and the shear-type idealisation (i.e., compatible with the Strong-Spandrels Weak-Piers (SSWP) in-plane global behaviour) but then also the Weak-Spandrels Strong-Piers (WSSP) behaviour as well as other intermediate behaviours may be described. The latter ones are obtained through the appropriate assignment of specific corrective factors (K_i, with i = 1 . . . 6) aimed at simulating the effects of various structural details (such as reinforced ring beams or tie-rods) on the lateral stiffness, the overall base shear, and the ultimate displacement capacity of the structure. Then, a nonlinear static procedure based on the use of over-damped spectra [52] is adopted to compute the value of the intensity measure that triggers each damage level while the uncertainty propagation due to the mechanical and

geometrical parameters (i.e., the structural capacity uncertainty) is explicitly accounted for through the response surface technique by assigning median values and dispersion capacities to them. Other sources of uncertainty (e.g., those associated with the seismic input or with the definition of the damage level) are instead included by assuming conventional a priori values for the dispersion, as derived from other evidence in the literature. This approach generates fragility functions that mainly refer to the in-plane global behaviour of URM buildings, but it considers the activation of out-of-plane (OOP) mechanisms too, in a simplified way, by limiting the displacement capacity through corrective coefficients based on expert judgment.

In the following paragraphs, a description of how each retrofit strategy was simulated by the three methods is provided.

3.2. Implementation of the Selected Retrofit Interventions within the Three Methods

Regarding the masonry strengthening interventions (MSN), both UniPD and UniGEb simulate these types of intervention by applying corrective coefficients to the mechanical characteristics of the materials, since they are explicitly accounted for in the methods. More specifically, these coefficients are assumed to start from those proposed in table C8.5.II of the Italian Technical Standard (Circular 21 January 2019) [43] and depend on the level of intervention (i.e., MSN1, MSN2 or MSN) and on the type of masonry. The corrective coefficients adopted in Vulnus vb 4.0 software and in DBV-Masonry are shown in Table 1. Despite the common source used by the two research units to retrieve the corrective coefficients, slightly different assumptions have been adopted to set the final values. In fact, UniPD coefficients average the values given for different types of material, whereas UniGEb uses, in the case of single interventions (i.e., MSN1), the coefficients proposed by the Italian Circular (21 January 2019) [43] and, in case of multiple simultaneous interventions (MSN2), the combined coefficients of the Italian Circular (21 January 2019) [43] but reduced by 10% to take into account the potential lower effectiveness of a combination of interventions. UniPD considered an average increase in the specific weight for masonry (5% in the case of stone masonry and 4% in the case of solid brick and hollow brick masonry), since the implemented interventions require the addition of material. In addition, the qualitative parameters of the GNDT level II form related to the masonry quality are improved as well. On the other hand, while deriving the capacity curve, the method proposed by UniGEb accounts for the potential impacts of various interventions on the increase in the global ductility for DS3 and DS4; the beneficial effects on the OOP mechanisms for irregular masonry; and, for solid and hollow brick masonry, the expected increase in the drift thresholds associated with reinforced concrete jackets or FRCM-TRM plasters.

Table 1. Corrective coefficients to simulate the masonry strengthening in the approaches adopted by UniPD and UniGEb.

Masonry Type		**Stone**				**Soft Stone**		**Solid Brick**	**Hollow Brick**
		Irregular	**Uncut**	**Cut**	**Ashlar**	**Irregular**	**Regular**		
MSN1	UniGEb	2	1.7	1.5	1.2	1.4	1.2	1.5	-
	UniPD	1.7				1.6		1.5	-
MSN2	UniGEb	2.9	2.3	1.9	1.2	1.4	1.2	1.6	-
	UniPD	2.4				1.9		1.8	-
MSN	UniGEb	2.9	2.3	1.9	1.2	1.4	1.2	1.6	1.3
	UniPD	-				-		1.7	1.3

Finally, according to the approach of UniGEa, the increase in the base shear capacity of the buildings is simulated by directly modifying the vulnerability V and ductility Q indices of the given vulnerability curves. The range of values presented in Table 2 corresponds to the variation in the modifiers varying the construction age and the number of storeys in the building. Negative values of ΔV correspond to a decrease in vulnerability.

Table 2. Vulnerability and ductility factors (V and Q) and modifiers (ΔV and ΔQ) used for the construction of as-built curves and for the simulation of the interventions in the approach adopted by UniGEa.

Construction Period		Pre-1919	1919–1945	1946–1960	1961–1970	1971–1980
As Built						
	V	0.92 ÷ 0.98	0.84 ÷ 0.91	0.71 ÷ 0.82	0.55 ÷ 0.65	0.51 ÷ 0.6
	Q	2.2 ÷ 2.4	2.4 ÷ 2.5	2.2 ÷ 2.4	2.2 ÷ 2.4	2.1 ÷ 2.4
Masonry strengthening						
MSN1	ΔV	−0.12 ÷ −0.135	−0.12	-	-	-
	ΔQ	0–−0.1	0 ÷ −0.1	-	-	-
MSN2	ΔV	−0.18 ÷ −0.225	−0.16 ÷ −0.2	-	-	-
	ΔQ	0–−0.2	0–−0.2	-	-	-
MSN	ΔV	-	-	−0.1 ÷ −0.135	−0.075	−0.05
	ΔQ	-	-	0–−0.1	0	0
Improvement of connections						
TR	ΔV	−0.05 ÷ −0.075	−0.05 ÷ −0.075	-	-	-
	ΔQ	0.2–0.3	0.1–0.2	-	-	-
CR	ΔV	-	-	−0.03 ÷ −0.05	0 ÷ −0.03	0
	ΔQ	-	-	0–0.1	0.1	0.1
Horizontal diaphragms stiffening						
FLR	ΔV	−0.1 ÷ −0.12	−0.075 ÷ −0.1	−0.05 ÷ −0.075	−0.03	−0.01
	ΔQ	0.2–0.3	0.2–0.3	0.1–0.2	0.1–0.2	0.1

The interventions used to improve connections (TRs and CRs) were also implemented differently by the three research units.

UniGEa simulated the effect of the addition of TRs through corrective coefficients for the ductility and vulnerability indices reported in Table 2, similar to what was conducted for the masonry reinforcement interventions.

UniPD implemented TRs directly in Vulnus, since it is possible to enter the number of TRs in both directions of the modelled building. In this study, the number of TRs that was adequate to prevent the activation of OOP mechanisms was added, i.e., two tie-rods for internal partitions and one tie-rod for each perimeter wall. Similarly, the CR intervention was simulated by placing two tie-rods in the two main directions of the building at each floor and at the roof level. In the case of these interventions, the associated GNDT level II form parameter was modified, too.

UniGEb instead implemented TRs in DBV-Masonry by adopting less penalizing corrective coefficients to the base shear and a lower rate was associated with the WSSP deformed shape, since it is expected that the seismic behaviour is moving to the SSWP solution. Moreover, less penalizing limitations for the displacement capacities of DS3 and DS4, by assuming that OOP mechanisms were prevented, were adopted, too. Analogously, the intervention with the insertion of confining-rings (CRs) aimed to ensure the box-like behaviour of the building by guaranteeing good coupling between the orthogonal walls and inhibiting the activation of OOP mechanisms; therefore, this type of intervention was expected to exploit the full displacement capacity of the structure without limitations.

Lastly, concerning the intervention of floor stiffening (FLR), none of the three methods directly modelled the floor stiffness.

Thus, to simulate FLR interventions, UniGEa once again modified the values of the vulnerability index and the ductility index according to Table 2.

Instead, the increased efficiency when distributing the horizontal actions given by FLR was simulated by UniPD in Vulnus inserting diffuse tie-rods, which increase the floor-to-wall friction coefficient and improve the qualitative parameters related to the floors

and roof. In the case of modern buildings, the friction coefficient was not increased, since it already had non-negligible values. In addition, in this case, an average increase in the floor specific weight by 1.2 kN/m^2 was estimated to consider the addition of new collaborating slabs.

Finally, the FLR intervention was implemented with the DBV-Masonry method by UniGEb considering different possible impacts according to the type of floor subjected to the intervention (i.e., wooden floors, vaulted floors, or floors with rigid or semi-rigid slab). Thus, the intervention produces the updating of the self-weight loads of floors and the modification of the corrective coefficients that simulate the prevailing global failure mechanism (i.e., SSWP or intermediate) and those that influence the ultimate displacement capacity (since the improvement in wall-to-diaphragm connections is expected to reduce the impact of OOP mechanisms, too).

With regard to combined interventions, whereas the models adopted by UniPD and UniGEb allow the simultaneous implementation of more than one intervention based on the aforementioned rules, the approach of UniGEa is based on the application of the modifiers shown in Table 2, which are combined according to the SRSS (Square Root of Sum of Squares) rule for the ΔV and the SUM rule for the ΔQ.

In addition to the specific differences in the implementation of the retrofit interventions, other general observations can be made. First, the UniPD method does not affect the distances among the fragility curves of the individual damage states, since Vulnus produces the fragility curve associated with DS2-3 damage that is later distributed over the five DSs (as specified in Section 3). Conversely, the UniGEb method can act on individual DSs by modifying their displacement capacities. In particular, for DS1 and DS2, this is a consequence of the variation in the yielding acceleration or the period and, for DS3 and DS4, the method acts on the corrective factors of the ductility or by modifying the drift capacities at the pier scale. The UniGEa model, on the other hand, modifies the distances among fragility curves of various DSs when an intervention is supposed to vary the Q index. Indeed, a variation in the slope of the vulnerability curve corresponds to a variation in the distance among the fragility curves.

4. Developed Fragility Models

4.1. ISTAT Types and Databases of Buildings Adopted for the Derivation of Fragility Curves

The three methods were adopted separately for the elaboration of three fragility models for the macro-classes of masonry buildings, both in their as-built condition and with the implementation of the retrofit interventions reported in Figure 1 of Section 2. On the basis of ISTAT census data [11] and in accordance with previous work [53], the ISTAT types are defined as the combination of five construction periods (i.e., pre-1919, 1919–1945, 1946–1960, 1961–1970, 1971–1980) and four height classes (1, 2, 3, and 4 or more storey buildings). Buildings designed after 1980 were excluded from this study, since they were taken as a reference for buildings designed according to more advanced technical standards and thus do not need retrofitting.

Following the macroseismic heuristic procedure reported in Section 3.1 [17], UniGEa calibrated the fragility sets of each ISTAT building type on the basis of the post-seismic damage data for residential masonry buildings hit by the 1980 Irpinia earthquake and the 2009 L'Aquila earthquake available from the AeDES forms collected in the Da.D.O. database [54]; these datasets were useful for calibrating the reference values of V and Q in the as-built state and the reference values of ΔV and ΔQ in the retrofitted state. UniPD instead collected a database of 445 buildings considered to be representative of the Italian residential masonry built heritage, both in terms of the variability with the geographical position and with respect to the typological variability in terms of the height and dimensions for each construction age. The buildings were collected from various surveys conducted by research groups of the University of Padova, whose designs refer to several Italian regions and municipalities, and their distribution within each construction period reflects the national one according to the ISTAT national census. In addition, the material properties

and the construction details were defined from the original designs or from the historical literature. For further details, please refer to [13,24]. All the buildings in the database were then modelled via Vulnus vb 4.0 software. Lastly, UniGEb first defined reference values for the mechanical and geometrical parameters that are explicitly involved in the computation of the capacity curves on the basis of a set of configurations representative of residential buildings available from some previous studies and then elaborated the fragility curves for the 120 branches obtained as a combination of the possible masonry, diaphragm, and structural detail typologies. For a given number of storeys, such branches were combined to pass to the ISTAT types by using the typological distribution of the residential buildings available in the Da.D.O database for the 2009 L'Aquila earthquake [54]. This last assumption is equivalent to consider—at least in the first instance—the residential building stock of the Abruzzi region that is representative for the whole country.

4.2. As-Built and Retrofitted Fragility Curves

The fragility models obtained for the ISTAT types for both the as-built and retrofit conditions are given in terms of the median μ and standard deviation β of the lognormal cumulative fragility curve presented in Appendix A: Tables A1–A5 list the UniGEa results; Tables A6–A9 report the UniPD curves, which are also described in more detail in [24]; and Tables A10–A13 contain the UniGEb model.

Figure 2 shows the fragility sets processed by the three research units for the analysed ISTAT building types in their as-built condition. The elaborated fragility curves are expressed in the form of the lognormal cumulative probability function; therefore, they can be described by the two parameters: the median and standard deviation. In the ISTAT types referring to construction periods before 1960 (pre-1919, 1919–1945, and 1946–1960), the fragility sets tend to be very consistent and comparable with each other, while greater variability can be seen for more recent construction periods (1961–1970 and 1971–1980). More substantial differences can also be noticed for higher damage states (DS4 and DS5), while a better match can be observed among the three research units for lower damage states (DS1, DS2, and DS3). This is motivated by the fact that high damage states, in particular, DS5, are difficult to reproduce numerically and are also observed empirically more rarely, resulting in greater variability among the fragility curves derived with different methods. Another feature that emerges from the graphs of Figure 2 is the greater dispersion (i.e., lower values of standard deviation, which result in flatter fragility curves) in the models of UniPD and UniGEa, which were both built starting from a macroseismic–heuristic model, while a lower dispersion is observed in the sets of UniGEb, consistent with the fact that it is a purely mechanical model.

Figures 3 and 4, respectively, show some examples of mitigated fragility sets for historical buildings and modern buildings. For graphical reasons, only the results for two-storey buildings are presented. This choice was made since the height class of the two-storey buildings is one of the most common in Italy, accounting for more than 50% of masonry buildings, according to ISTAT [11].

Similar to the as-built cases, good correspondence between the three models can be observed, especially for the fragility curves of lower damage states and for the oldest ISTAT types. Additionally, it can be noticed that the DSs are not all equally distributed in the different methods, even when they refer to the same seismic retrofit intervention. This difference is clear, for example, for the fragility sets related to the interventions applied to modern construction ages (Figure 4), in which DS3 and DS4 of the UniGEb model are very close to each other, while the UniPD and UniGEa models maintain a more uniform damage distribution. This originates from the differences in the applied methods already illustrated in Section 3.2.

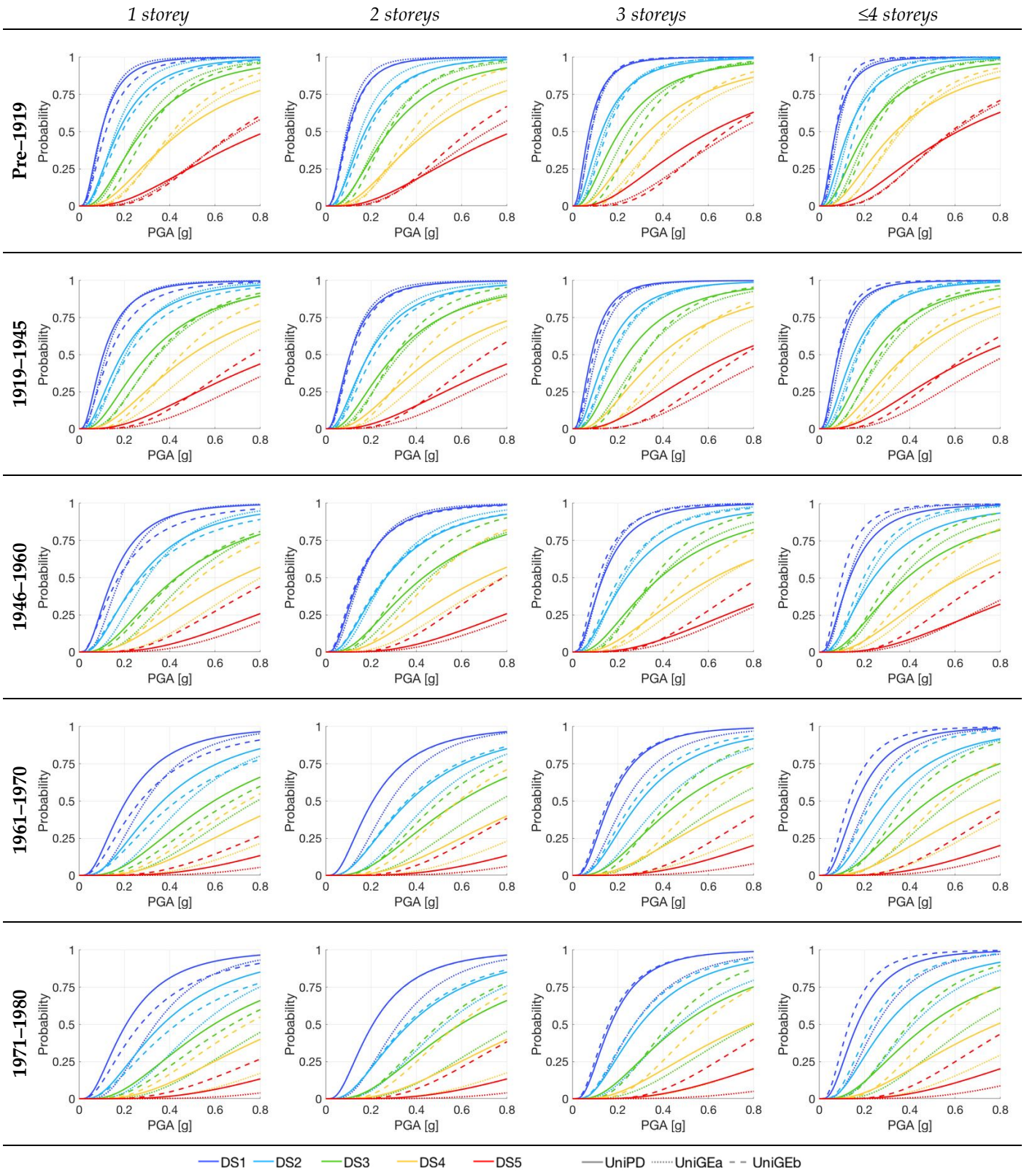

Figure 2. Fragility sets of the as-built configuration for the pre-1919, 1946–1960, and 1971–1980 periods.

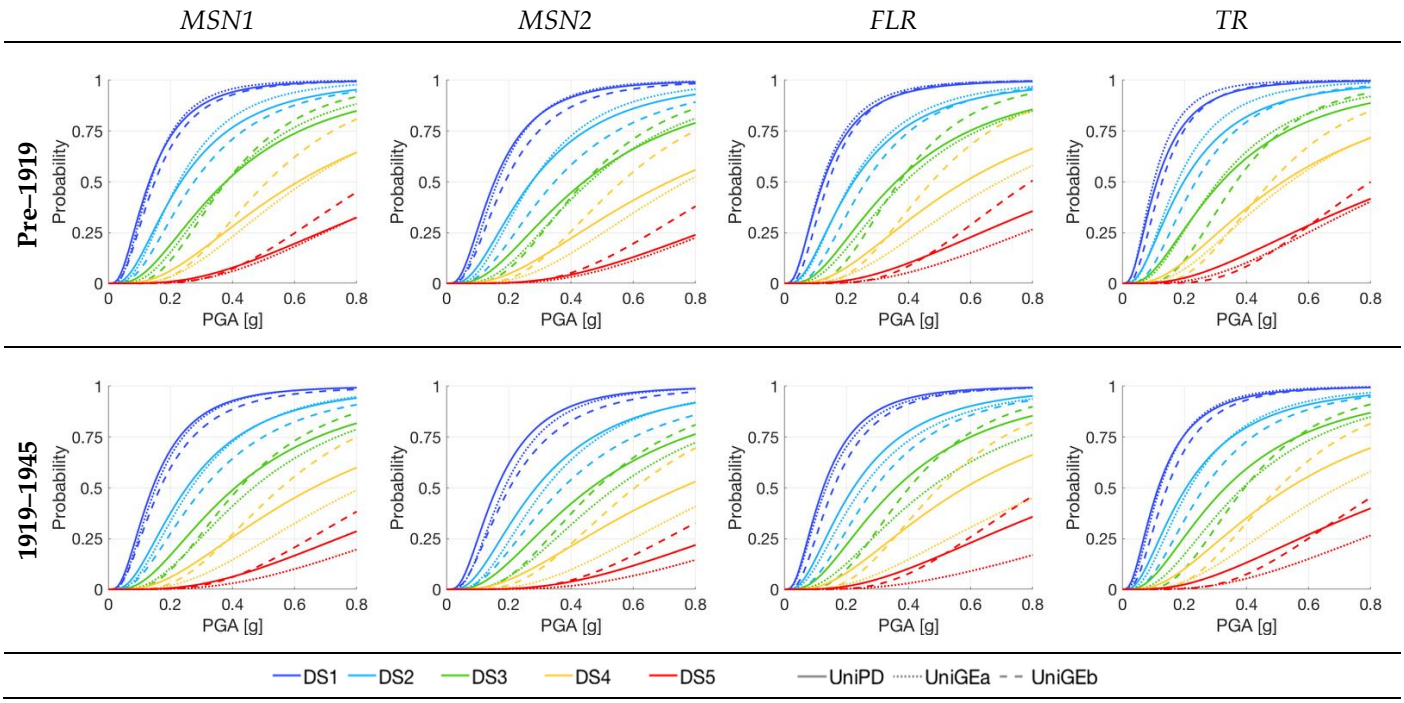

Figure 3. Fragility sets of two-storey retrofitted masonry buildings pre-1919 and for 1919–1945.

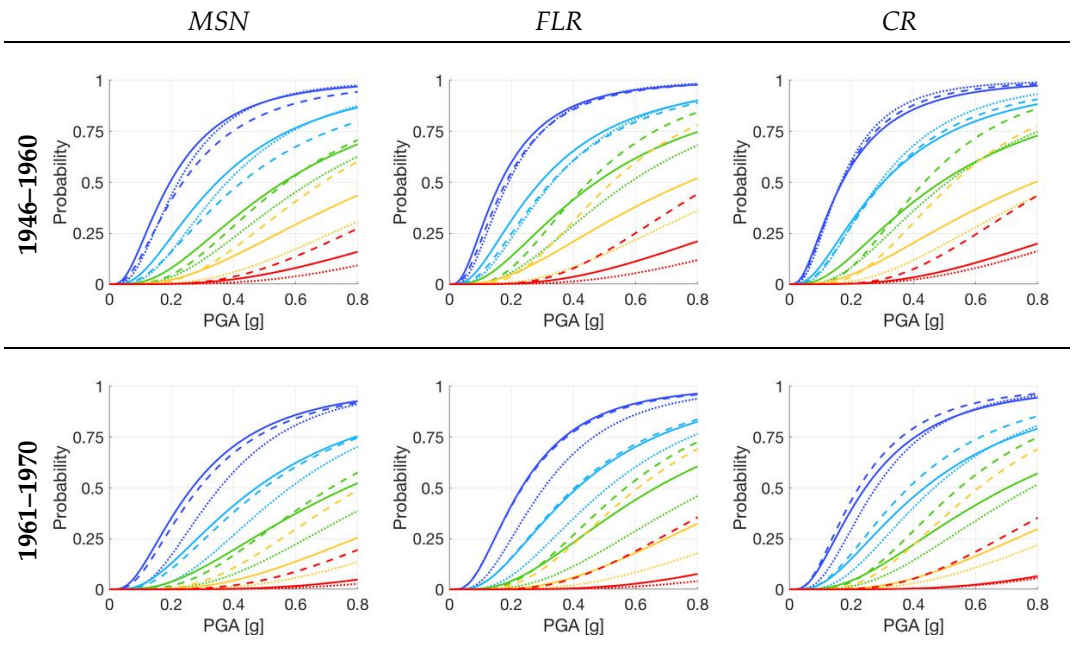

Figure 4. *Cont.*

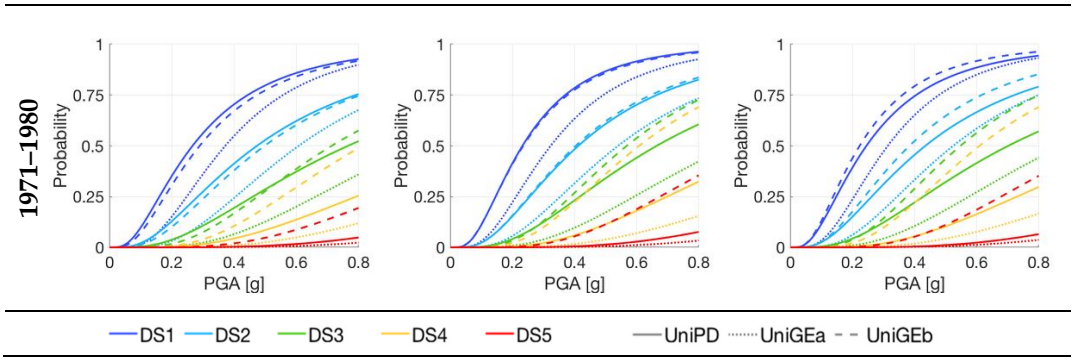

Figure 4. Fragility sets of two-storey retrofitted masonry buildings for 1946–1960, 1961–1970, and 1971–1980.

5. Effectiveness of Interventions

The fragility sets presented so far allow an immediate visual representation and comparison among the three proposed models. However, they do not allow the increase in building performance, i.e., the difference in damage states between the mitigated and the as-built fragility curves, to be captured. This section is therefore dedicated to some model comparisons, in terms of the percentage increase in the median PGA of the retrofitted fragility curves from the as-built ones. These results are shown in the histograms presented in Figures 5–9 (for DS1, DS3, and DS5), and they can be seen as a graphical representation of how much a particular intervention improves the seismic behaviour of the building compared to the as-built state.

Since each research unit has produced its own as-built fragility set, these results should be read in relative (not absolute) terms for the vulnerability reduction. Nevertheless, this representation is particularly useful when comparing different fragility models because it allows an evaluation of the actual performance increase recorded by each model, regardless of the initial as-built vulnerability.

The images confirm the consistency of the results among different models: even when an intervention leads to different improvements according to different methods, the efficiency (percentage increase of PGA) is usually confirmed among the interventions. Another feature that emerges from the graphs is the lower effectiveness of the interventions in more recent construction periods (with a maximum percentage increase in the median PGA of 60% for post-1960 construction periods) compared to historical ones (percentage increase in the median PGA which can reach 180% for the pre-1919 epoch), an outcome that was expected and can be justified by the fact that, in the case of modern ISTAT types, the as-built condition already presents a more adequate seismic performance in the as-built state.

Other than individual interventions, the performance increase in the case of combined interventions is also shown in Figures 5–9. It is worth highlighting that combined interventions are always more effective than the corresponding individual ones, although their improvement is not necessarily the sum of the improvements given by the two individual interventions. As an example, we can observe that masonry strengthening interventions are more effective than interventions aimed at improving the connections and the horizontal diaphragm stiffness. Indeed, the addition of ties or the floor stiffening in historic buildings improves their behaviour against out-of-plane wall overturning and favours a better load distribution among shear walls. These improvements are caught by all fragility models; however, when they are implemented, if the masonry strength is not concurrently improved, failure occurs on the walls for a low level of action, and this condition hinders a more significant reduction in vulnerability. Similarly, the improvement in the masonry strength appears to be very effective, but when it is carried out alone, it does not prevent out-of-plane wall overturning, nor does it cause a better distribution of shear among the resisting walls. Thus, when both classes of interventions are carried out together, the over-

all performance increase is often higher than those given by the individual interventions alone, especially for the UniPD and UniGEb models. This can be observed, for example, in the DS3 of the pre-1919 buildings with two storeys: the MNS2 intervention produces percentage increases in the median PGA of 80% for UniGEa, 58% for UniPD, and 62% for UniGEb, whereas the TR intervention gives percentage increases in the median PGA of 21%, 14%, and 32% for UniGEa, UniPD, and UniGEb, respectively. The simple sum of the contribution of the two interventions MSN2 + TR gives 101% (UniGEa), 72% (UniPD), and 96% (UniGEb); however, the results obtained from the analysis are 92% (UniGEa), 95% (UniPD), and 111% (UniGEb).

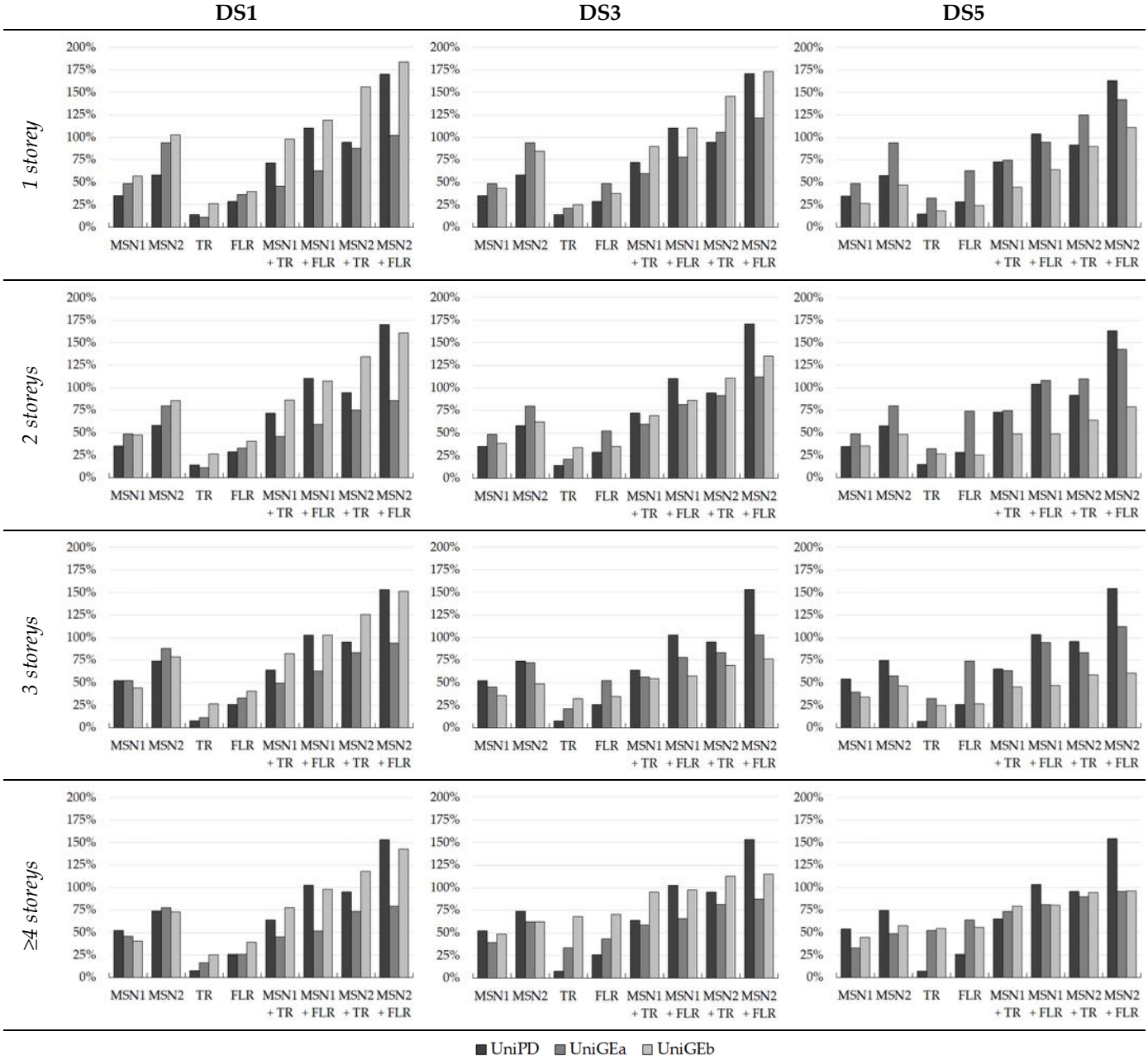

Figure 5. Percentage increases in the median PGA of the DS1, DS3, and DS5 fragility curves for pre-1919 buildings with interventions.

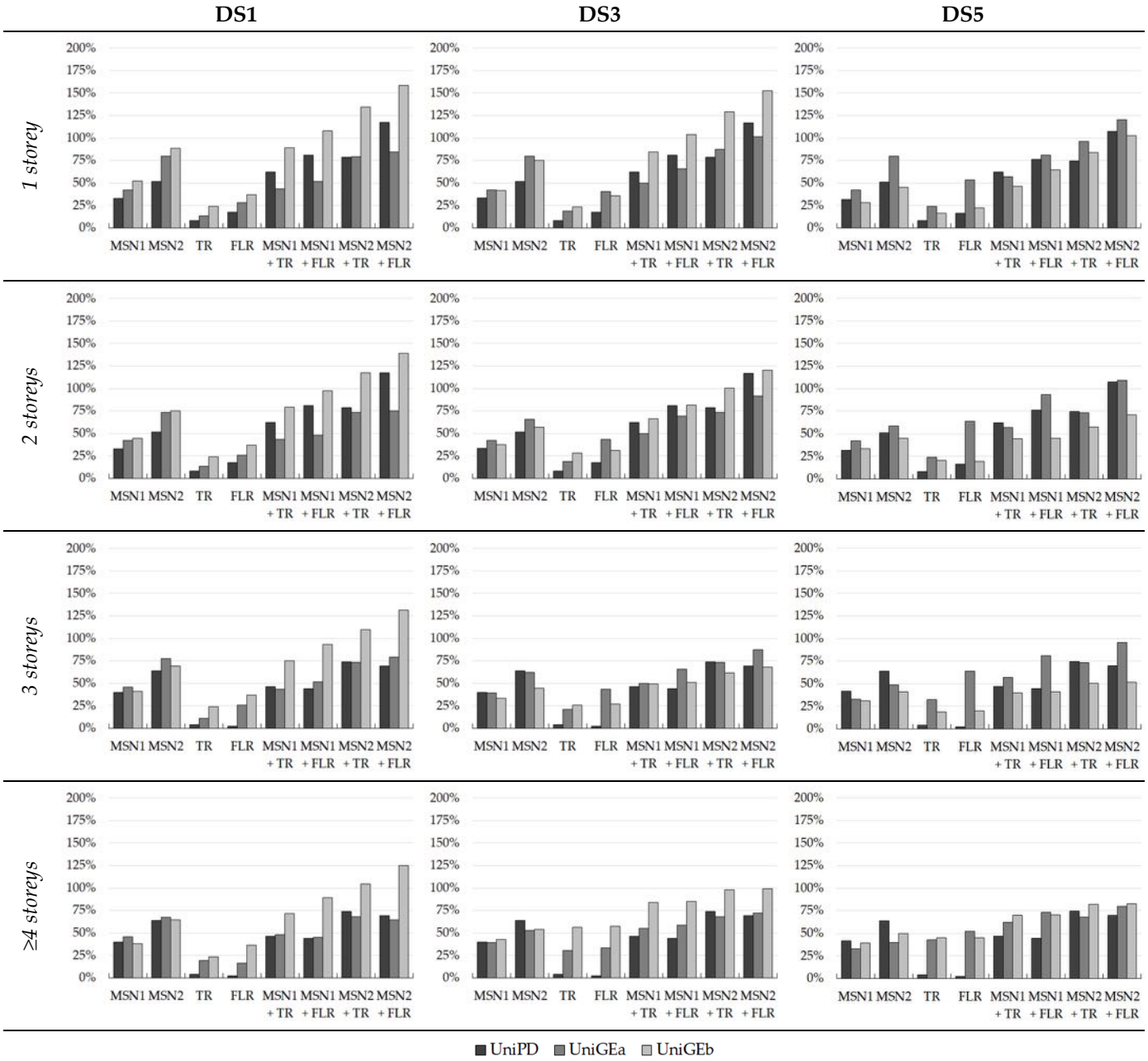

Figure 6. Percentage increases in the median PGA of the DS1, DS3, and DS5 fragility curves for 1919–1945 buildings with interventions.

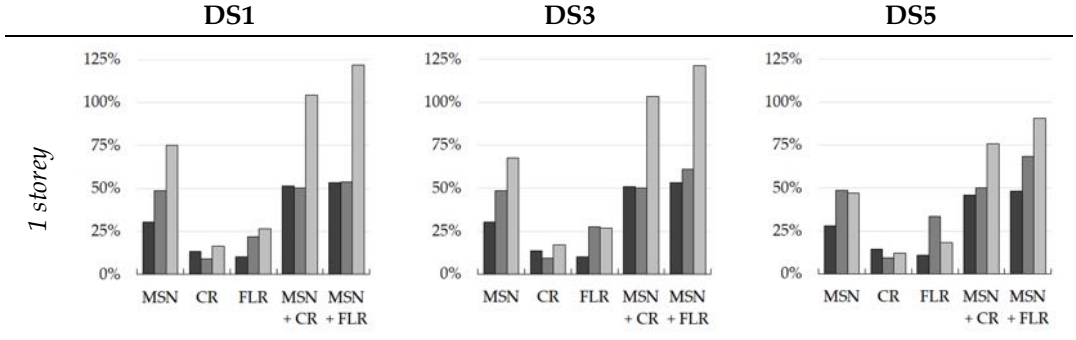

Figure 7. *Cont.*

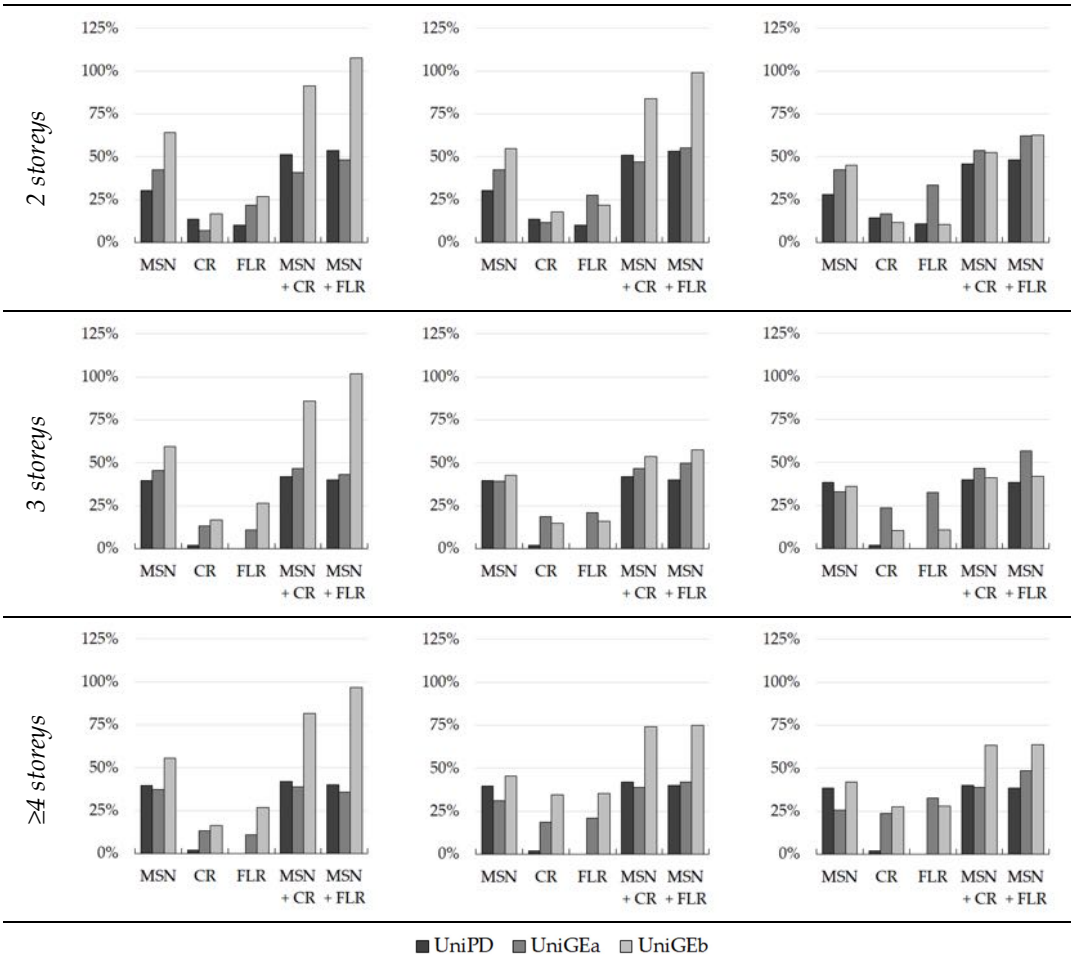

Figure 7. Percentage increases in the median PGA of the DS1, DS3, and DS5 fragility curves for 1946–1960 buildings with interventions.

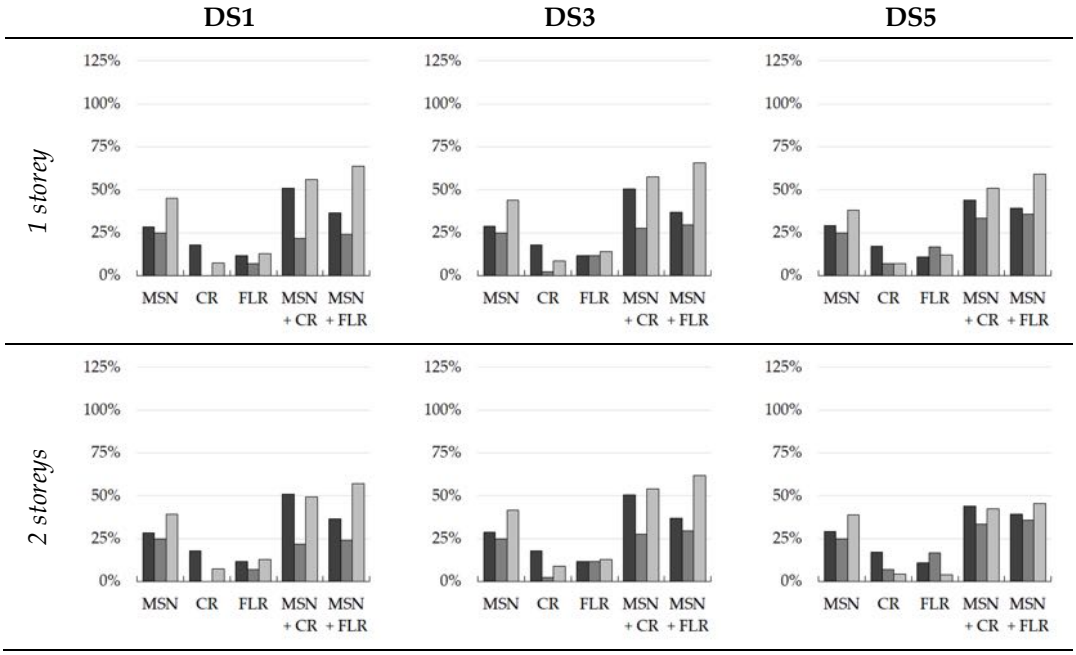

Figure 8. *Cont.*

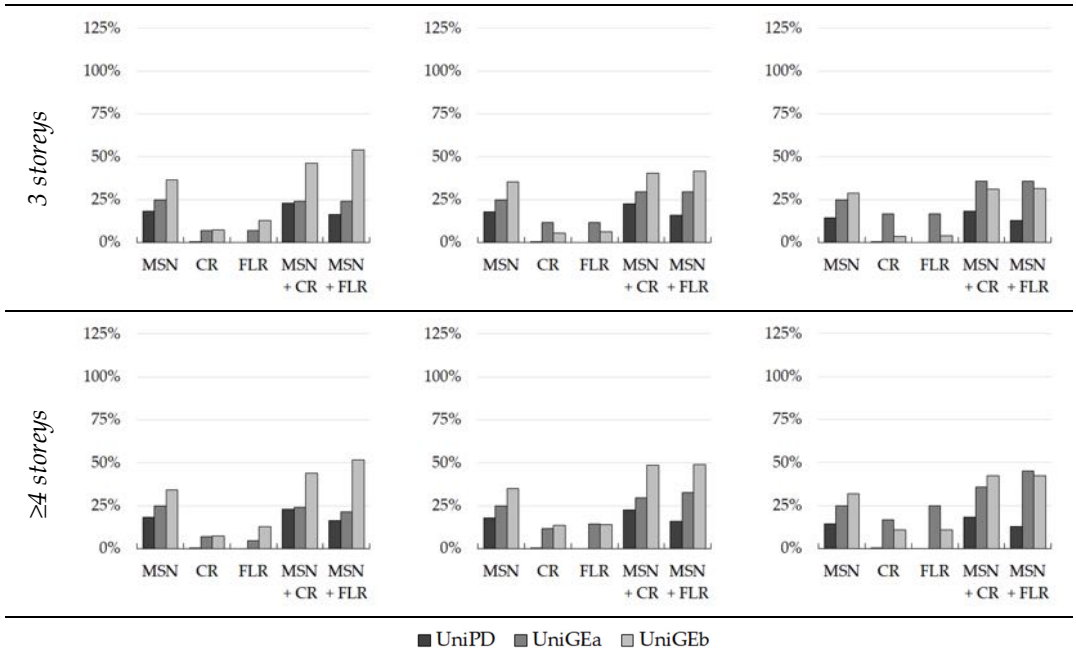

Figure 8. Percentage increases in the median PGA of the DS1, DS3, and DS5 fragility curves for 1961–1970 buildings with interventions.

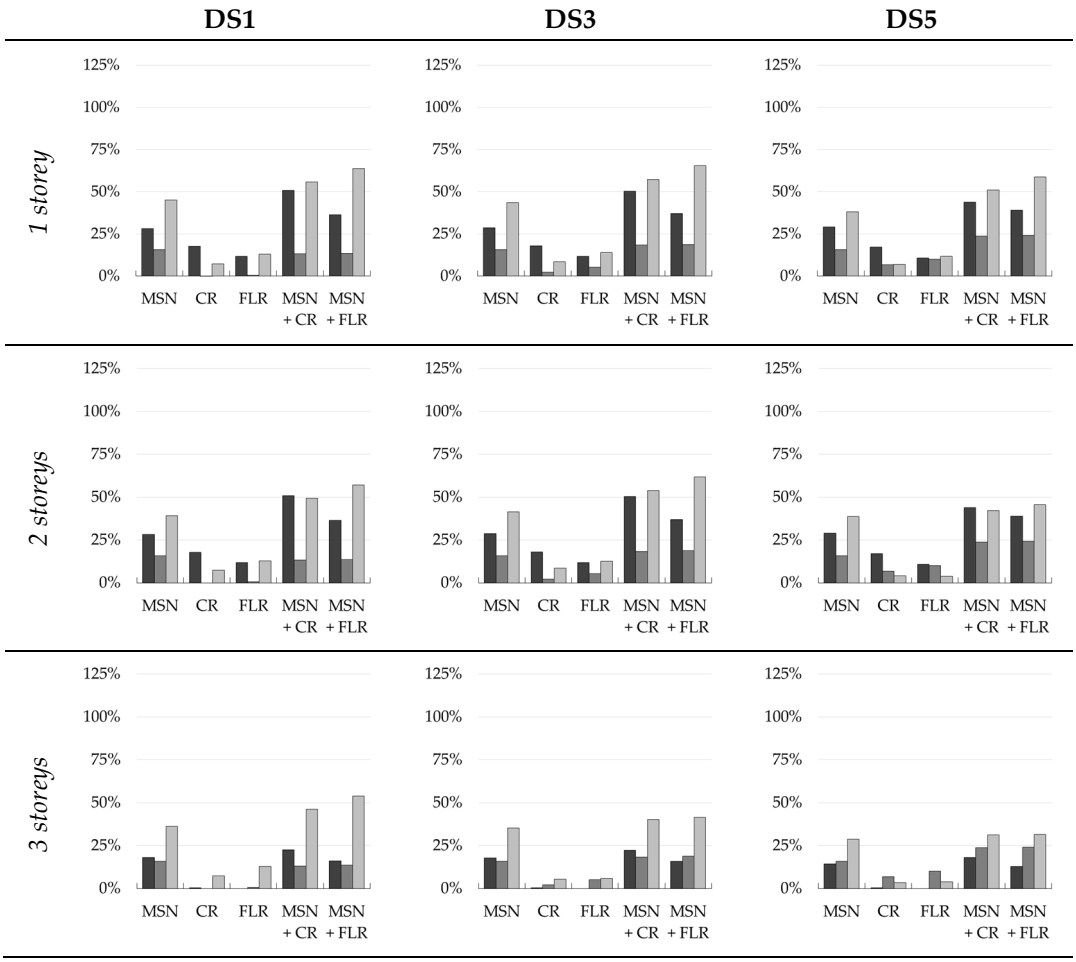

Figure 9. *Cont.*

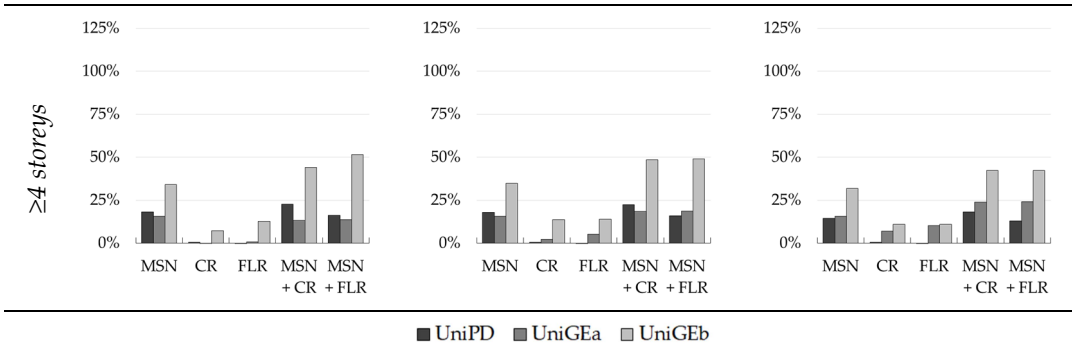

Figure 9. Percentage increases in the median PGA of the DS1, DS3, and DS5 fragility curves for 1971–1980 buildings with interventions.

Figure 10 shows the percentage increases in performance that have previously been presented, providing a more direct comparison among the DSs for the three models. The observations made earlier in Section 4.2 about the different distributions of DSs for the different methods are shown here with a graphical representation. In particular, it appears that the DSs of different retrofitted models, even when they are referring to the same intervention, do not always experience the same increase in the median PGA. For example, it can be noticed that the UniPD model does not significantly capture any differences among DSs, because the method is processed starting from an intermediate DS, and then extended to the other DSs. For UniGEa, interventions seem to be more effective for high than for low damage states when they improve the box-like behaviour of buildings (i.e., TR/CR and FLR), while they have the same effectiveness for all DSs when they increase the masonry strength and quality (i.e., MSN2/MSN). Lastly, in the histograms representing the UNIGEb results, interventions have an overall stronger influence on lower DSs (DS1–DS2) than on higher DSs (DS4–DS5). The different percentage increase in the PGA among the DSs can be seen as the effect that interventions have on the ductility of the structure. In this representation, the ductility of the structure can be observed in the distance between curves representing different DSs (width of the fragility set). In fact, if the required increase in the PGA to switch from one DS to the following one is small, once a low DS is reached, a small increase in acceleration will be enough to reach more severe damage states (brittle behaviour). On the other hand, if the PGA increase needs to be high to switch from one DS to the next, the building can be deemed to have ductile behaviour.

As mentioned above, these differences are derived from the methods used: macroseismic–heuristic in the case of UNIGEa and purely mechanical in the case of UNIGEb.

From the presented histograms, besides the differences according to the type of intervention, some other differences can be noticed depending on the construction period. As an example, among the individual (not combined) retrofit solutions, the interventions on masonry (MSN1, MSN2 and MSN) have a stronger influence on the building fragility. However, this effect decreases as the construction period becomes more recent, and this is reasonable considering that historical buildings are composed of masonry of poorer quality, whereas modern masonry already has almost satisfactory resistance.

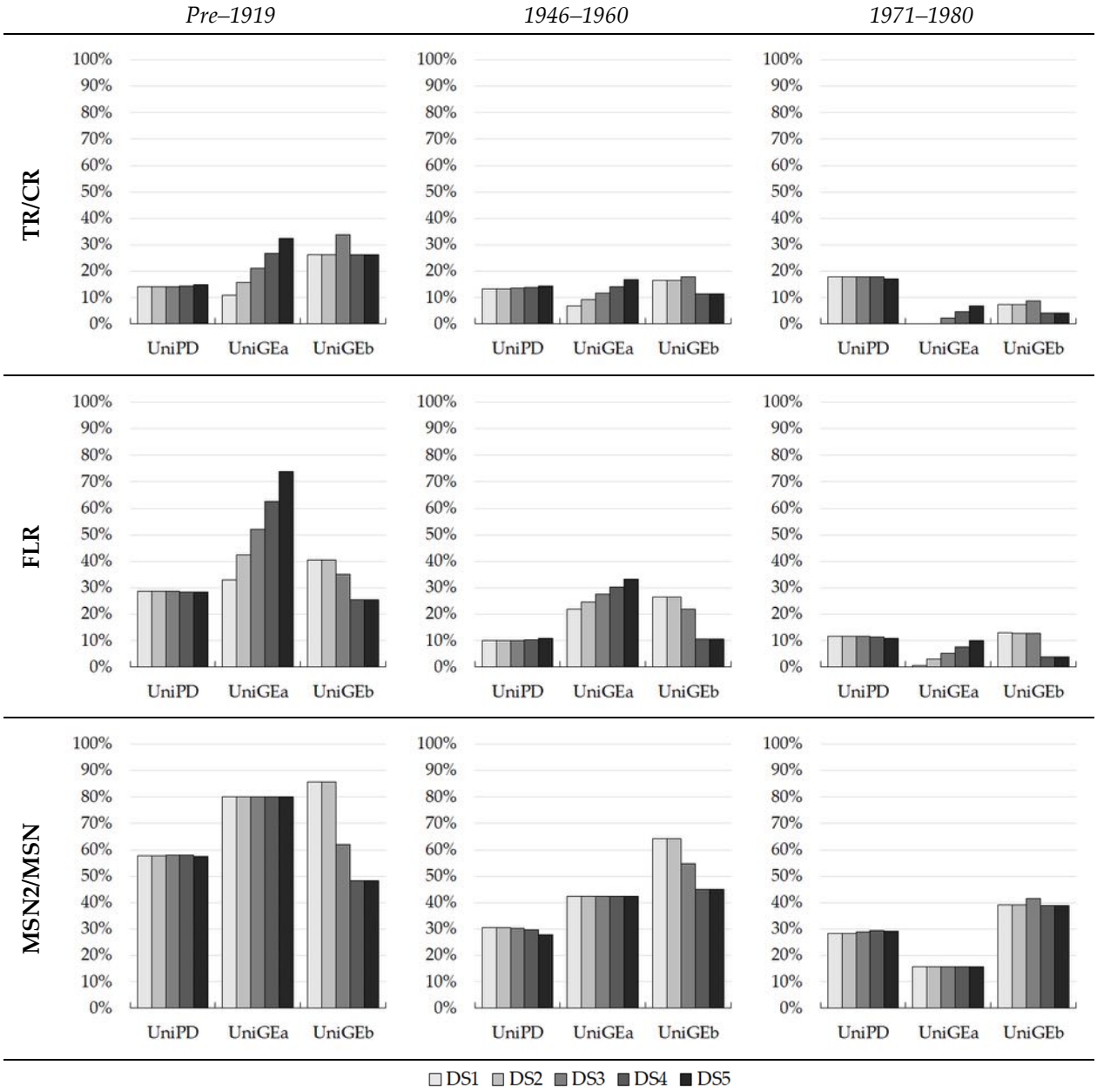

Figure 10. Percentage increases in the median PGA of the DS1–DS5 fragility curves compared to the as-built curves of two-storey buildings from three different construction periods (pre-1919, 1946–1960, 1971–1980) for the TR/CR, FLR, and MSN2/MSN interventions.

6. Conclusions

This study presents three approaches for the vulnerability assessment of masonry structures used by UniPD, UniGEa, and UniGEb as part of the ReLUIS-MARS project. In particular, UniGEa proposed the use of a macroseismic–heuristic model applied to residential buildings collected in the Da.D.O. database, defining modifiers to model the effectiveness of the interventions; UniPD developed a simplified mechanical–heuristic procedure based on the implementation of a database of buildings in Vulnus; lastly, UniGEb elaborated on a mechanical procedure using the DBV-Masonry approach.

Three categories of retrofit solutions were selected and modelled: masonry strengthening (MSN1, MSN2, MSN), connection improvement (TR/CR), and floor stiffening (FLR). The research units simulated and implemented each intervention through their methods to

create a final fragility model for various building macro-classes that represent the Italian stock of residential masonry buildings.

The obtained results show the seismic improvement that each intervention strategy brings to the various building macro-classes, in particular:

- The best-performing interventions are those of masonry strengthening (MSN2, MSN) for all of the construction periods analysed with a decreasing effectiveness as the age of the building decreases (i.e., for the more recent construction periods);
- Referring to DS3 (shown in Figure 10) and considering an average value among the results from the three methodologies, average percentage increases in the median PGA of 67% for pre-1919, 42% for 1946–1960, and 29% for 1971–1980 can be observed in the case of masonry strengthening;
- Concerning floor stiffening (FLR) interventions and to improve the box-like behaviour of the building by means of tie-rods (TR) or confining-rings (CR), it can be observed that, in this case, their effectiveness has the tendency to decrease as the age of the building decreases;
- For these interventions, the average increase in the DS3 median PGA is 39% for pre-1919, 20% for 1946–1960, and 10% for 1971–1980 for the FLR intervention, and 23% for pre-1919, 14% for 1946–1960, and 10% for 1971–1980 for the TR/CR interventions;
- As a summary for all types of strengthening, it can be said that FLR interventions drastically improve the seismic responses of more ancient buildings due to the poor performance of their original floors, while the effectiveness of this kind of intervention noticeably decreases in newer buildings. TR and CR interventions demonstrate more consistent behaviour in terms of improving the seismic performance of masonry buildings, despite having a minor effectiveness decrease throughout the different construction periods. Lastly, masonry strengthening interventions maintain high effectiveness, even in recent construction periods;
- The combined application of more interventions is always more efficient than the application of the individual interventions;
- The results presented by a percentage increase in the performance brought by different interventions for different building macro-classes obtained with the three methods confirmed the previous results and allowed the three methods to be compared;
- Although the results of the three models are different, due to their different approaches, the mitigated fragility sets display similar trends in terms of the improvements brought by the interventions, mutually validating the reliability of the three proposed models.

This paper offers some useful results regarding the evaluation of the effectiveness of different retrofit approaches for defining risk mitigation strategies. Despite the important contribution of this work, for a complete risk assessment and the planning of mitigation strategies, further research might be carried out. Potential future developments of this work may include the analysis of additional retrofit interventions for the building macro-classes presented in this work, including the combination of multiple interventions. Furthermore, cost–benefit analyses will be carried out considering the cost of the interventions and their effectiveness to produce trade-off maps that will help risk management authorities to select and plan the best mitigation strategies.

Author Contributions: Conceptualisation, methodology, supervision and resources: S.C., F.d.P., M.D. and S.L.; formal analysis, data curation and visualisation: S.A., P.C. and V.F.; writing—original draft preparation: P.C. and V.F.; writing—review and editing: S.A., S.C. and F.d.P. All authors have read and agreed to the published version of the manuscript.

Funding: This research received no external funding.

Data Availability Statement: Data is contained within the article and Appendix A.

Acknowledgments: Special thanks are given to the Italian Department of Civil Protection (DPC), which funded this study under the framework of the ReLUIS-DPC Project 2019–2021—Work Package 4: MARS (MAps of Risk and Scenarios of seismic damage)—Task 6: Preventive strategies.

Conflicts of Interest: The authors declare no conflict of interest.

Appendix A

Table A1. μ (median) and β (standard deviation) values of the as-built and retrofitted fragility models of UniGEa, for pre-1919 masonry buildings.

Pre-1919			DS1		DS2		DS3		DS4		DS5	
Id	**N. Storeys**	**Intervention**	**μ [g]**	**β [-]**	**μ [g]**	**β [-]**	**μ [g]**	**β [-]**	**μ [g]**	**β [-]**	**μ [g]**	**β [-]**
1	1	AS-BUILT	0.099	0.600	0.162	0.600	0.265	0.600	0.433	0.600	0.708	0.600
2	1	MSN1	0.147	0.600	0.241	0.600	0.394	0.600	0.644	0.600	1.052	0.600
3	1	MSN2	0.192	0.600	0.314	0.600	0.513	0.600	0.839	0.600	1.371	0.600
4	1	TR	0.110	0.650	0.188	0.650	0.321	0.650	0.548	0.650	0.937	0.650
5	1	FLR	0.135	0.650	0.231	0.650	0.394	0.650	0.673	0.650	1.151	0.650
6	1	MSN1 + TR	0.145	0.650	0.247	0.650	0.423	0.650	0.723	0.650	1.235	0.650
7	1	MSN1 + FLR	0.161	0.650	0.275	0.650	0.471	0.650	0.805	0.650	1.376	0.650
8	1	MSN2 + TR	0.187	0.650	0.319	0.650	0.545	0.650	0.932	0.650	1.593	0.650
9	1	MSN2 + FLR	0.201	0.650	0.343	0.650	0.586	0.650	1.001	0.650	1.712	0.650
10	2	AS-BUILT	0.091	0.625	0.153	0.625	0.255	0.625	0.427	0.625	0.713	0.625
11	2	MSN1	0.136	0.625	0.227	0.625	0.380	0.625	0.635	0.625	1.061	0.625
12	2	MSN2	0.164	0.625	0.275	0.625	0.460	0.625	0.768	0.625	1.284	0.625
13	2	TR	0.101	0.675	0.177	0.675	0.309	0.675	0.541	0.675	0.945	0.675
14	2	FLR	0.122	0.700	0.217	0.700	0.388	0.700	0.694	0.700	1.241	0.700
15	2	MSN1 + TR	0.133	0.675	0.233	0.675	0.408	0.675	0.712	0.675	1.245	0.675
16	2	MSN1 + FLR	0.145	0.700	0.260	0.700	0.464	0.700	0.830	0.700	1.483	0.700
17	2	MSN2 + TR	0.160	0.675	0.280	0.675	0.489	0.675	0.855	0.675	1.495	0.675
18	2	MSN2 + FLR	0.170	0.700	0.303	0.700	0.542	0.700	0.969	0.700	1.731	0.700
19	3	AS-BUILT	0.084	0.650	0.144	0.650	0.246	0.650	0.421	0.650	0.719	0.650
20	3	MSN1	0.128	0.625	0.214	0.625	0.358	0.625	0.598	0.625	1.000	0.625
21	3	MSN2	0.159	0.600	0.259	0.600	0.424	0.600	0.693	0.600	1.132	0.600
22	3	TR	0.093	0.700	0.167	0.700	0.298	0.700	0.533	0.700	0.953	0.700
23	3	FLR	0.112	0.725	0.205	0.725	0.375	0.725	0.685	0.725	1.251	0.725
24	3	MSN1 + TR	0.126	0.675	0.220	0.675	0.384	0.675	0.672	0.675	1.174	0.675
25	3	MSN1 + FLR	0.137	0.700	0.245	0.700	0.438	0.700	0.782	0.700	1.398	0.700
26	3	MSN2 + TR	0.154	0.650	0.264	0.650	0.451	0.650	0.771	0.650	1.318	0.650
27	3	MSN2 + FLR	0.164	0.675	0.286	0.675	0.500	0.675	0.873	0.675	1.526	0.675
28	≥4	AS-BUILT	0.083	0.600	0.136	0.600	0.222	0.600	0.363	0.600	0.593	0.600
29	≥4	MSN1	0.121	0.575	0.193	0.575	0.309	0.575	0.494	0.575	0.789	0.575
30	≥4	MSN2	0.147	0.550	0.231	0.550	0.360	0.550	0.563	0.550	0.880	0.550
31	≥4	TR	0.097	0.675	0.169	0.675	0.296	0.675	0.517	0.675	0.904	0.675
32	≥4	FLR	0.104	0.675	0.182	0.675	0.318	0.675	0.557	0.675	0.973	0.675
33	≥4	MSN1 + TR	0.120	0.650	0.206	0.650	0.352	0.650	0.601	0.650	1.028	0.650
34	≥4	MSN1 + FLR	0.126	0.650	0.215	0.650	0.367	0.650	0.628	0.650	1.073	0.650
35	≥4	MSN2 + TR	0.144	0.625	0.241	0.625	0.403	0.625	0.673	0.625	1.125	0.625
36	≥4	MSN2 + FLR	0.149	0.625	0.249	0.625	0.416	0.625	0.695	0.625	1.162	0.625

Table A2. μ (median) and β (standard deviation) values of the as-built and retrofitted fragility models of UniGEa for 1919–1945 masonry buildings.

1919–1945			DS1		DS2		DS3		DS4		DS5	
Id	**N. Storeys**	**Intervention**	**μ [g]**	**β [-]**	**μ [g]**	**β [-]**	**μ [g]**	**β [-]**	**μ [g]**	**β [-]**	**μ [g]**	**β [-]**
37	1	AS-BUILT	0.120	0.650	0.205	0.650	0.350	0.650	0.599	0.650	1.023	0.650
38	1	MSN1	0.171	0.650	0.292	0.650	0.498	0.650	0.852	0.650	1.456	0.650
39	1	MSN2	0.216	0.650	0.369	0.650	0.631	0.650	1.078	0.650	1.842	0.650
40	1	TR	0.136	0.675	0.237	0.675	0.415	0.675	0.725	0.675	1.268	0.675
41	1	FLR	0.154	0.700	0.275	0.700	0.491	0.700	0.878	0.700	1.570	0.700
42	1	MSN1 + TR	0.172	0.675	0.300	0.675	0.525	0.675	0.917	0.675	1.604	0.675

Table A2. *Cont.*

1919–1945			DS1		DS2		DS3		DS4		DS5	
Id	**N. Storeys**	**Intervention**	**μ [g]**	**β [-]**	**μ [g]**	**β [-]**	**μ [g]**	**β [-]**	**μ [g]**	**β [-]**	**μ [g]**	**β [-]**
43	1	MSN1 + FLR	0.181	0.700	0.324	0.700	0.580	0.700	1.036	0.700	1.852	0.700
44	1	MSN2 + TR	0.215	0.675	0.376	0.675	0.657	0.675	1.148	0.675	2.006	0.675
45	1	MSN2 + FLR	0.221	0.700	0.395	0.700	0.707	0.700	1.263	0.700	2.258	0.700
46	2	AS-BUILT	0.107	0.675	0.188	0.675	0.328	0.675	0.573	0.675	1.002	0.675
47	2	MSN1	0.153	0.675	0.267	0.675	0.467	0.675	0.816	0.675	1.426	0.675
48	2	MSN2	0.186	0.650	0.318	0.650	0.544	0.650	0.930	0.650	1.590	0.650
49	2	TR	0.122	0.700	0.217	0.700	0.388	0.700	0.694	0.700	1.241	0.700
50	2	FLR	0.135	0.750	0.252	0.750	0.471	0.750	0.879	0.750	1.644	0.750
51	2	MSN1 + TR	0.154	0.700	0.275	0.700	0.491	0.700	0.878	0.700	1.570	0.700
52	2	MSN1 + FLR	0.159	0.750	0.297	0.750	0.555	0.750	1.037	0.750	1.939	0.750
53	2	MSN2 + TR	0.186	0.675	0.325	0.675	0.568	0.675	0.993	0.675	1.735	0.675
54	2	MSN2 + FLR	0.188	0.725	0.344	0.725	0.628	0.725	1.148	0.725	2.098	0.725
55	3	AS-BUILT	0.107	0.650	0.182	0.650	0.311	0.650	0.532	0.650	0.910	0.650
56	3	MSN1	0.155	0.625	0.259	0.625	0.433	0.625	0.724	0.625	1.211	0.625
57	3	MSN2	0.189	0.600	0.309	0.600	0.506	0.600	0.826	0.600	1.351	0.600
58	3	TR	0.118	0.700	0.211	0.700	0.377	0.700	0.674	0.700	1.205	0.700
59	3	FLR	0.134	0.725	0.244	0.725	0.447	0.725	0.817	0.725	1.493	0.725
60	3	MSN1 + TR	0.153	0.675	0.267	0.675	0.467	0.675	0.816	0.675	1.426	0.675
61	3	MSN1 + FLR	0.161	0.700	0.288	0.700	0.515	0.700	0.921	0.700	1.647	0.700
62	3	MSN2 + TR	0.185	0.650	0.316	0.650	0.539	0.650	0.922	0.650	1.576	0.650
63	3	MSN2 + FLR	0.191	0.675	0.334	0.675	0.583	0.675	1.020	0.675	1.782	0.675
64	≥4	AS-BUILT	0.098	0.650	0.167	0.650	0.285	0.650	0.487	0.650	0.833	0.650
65	≥4	MSN1	0.142	0.625	0.237	0.625	0.397	0.625	0.663	0.625	1.109	0.625
66	≥4	MSN2	0.163	0.600	0.267	0.600	0.436	0.600	0.713	0.600	1.166	0.600
67	≥4	TR	0.116	0.700	0.208	0.700	0.372	0.700	0.664	0.700	1.187	0.700
68	≥4	FLR	0.114	0.725	0.208	0.725	0.380	0.725	0.695	0.725	1.270	0.725
69	≥4	MSN1 + TR	0.145	0.675	0.253	0.675	0.442	0.675	0.773	0.675	1.350	0.675
70	≥4	MSN1 + FLR	0.141	0.700	0.253	0.700	0.452	0.700	0.808	0.700	1.444	0.700
71	≥4	MSN2 + TR	0.164	0.650	0.280	0.650	0.479	0.650	0.819	0.650	1.400	0.650
72	≥4	MSN2 + FLR	0.160	0.675	0.280	0.675	0.490	0.675	0.857	0.675	1.497	0.675

Table A3. μ (median) and β (standard deviation) values of the as-built and retrofitted fragility models of UniGEa for 1946–1960 masonry buildings.

1946–1960			DS1		DS2		DS3		DS4		DS5	
Id	**N. Storeys**	**Intervention**	**μ [g]**	**β [-]**	**μ [g]**	**β [-]**	**μ [g]**	**β [-]**	**μ [g]**	**β [-]**	**μ [g]**	**β [-]**
73	1	AS-BUILT	0.184	0.600	0.300	0.600	0.491	0.600	0.802	0.600	1.312	0.600
74	1	MSN	0.273	0.600	0.447	0.600	0.730	0.600	1.193	0.600	1.950	0.600
75	1	CR	0.201	0.600	0.328	0.600	0.536	0.600	0.876	0.600	1.432	0.600
76	1	FLR	0.224	0.625	0.374	0.625	0.626	0.625	1.046	0.625	1.748	0.625
77	1	MSN + CR	0.276	0.600	0.451	0.600	0.737	0.600	1.205	0.600	1.969	0.600
78	1	MSN + FLR	0.283	0.625	0.473	0.625	0.790	0.625	1.321	0.625	2.208	0.625
79	2	AS-BUILT	0.156	0.650	0.267	0.650	0.456	0.650	0.780	0.650	1.333	0.650
80	2	MSN	0.222	0.650	0.380	0.650	0.649	0.650	1.110	0.650	1.897	0.650
81	2	CR	0.167	0.675	0.292	0.675	0.510	0.675	0.891	0.675	1.557	0.675
82	2	FLR	0.190	0.675	0.333	0.675	0.582	0.675	1.017	0.675	1.777	0.675
83	2	MSN + CR	0.220	0.675	0.384	0.675	0.671	0.675	1.173	0.675	2.051	0.675
84	2	MSN + FLR	0.232	0.675	0.405	0.675	0.707	0.675	1.236	0.675	2.161	0.675
85	3	AS-BUILT	0.131	0.650	0.224	0.650	0.383	0.650	0.654	0.650	1.118	0.650
86	3	MSN	0.191	0.625	0.318	0.625	0.532	0.625	0.890	0.625	1.487	0.625
87	3	CR	0.148	0.675	0.259	0.675	0.453	0.675	0.792	0.675	1.384	0.675
88	3	FLR	0.145	0.700	0.259	0.700	0.463	0.700	0.828	0.700	1.480	0.700

Table A3. *Cont.*

1946–1960			DS1		DS2		DS3		DS4		DS5	
Id	**N. Storeys**	**Intervention**	**μ [g]**	**β [-]**	**μ [g]**	**β [-]**	**μ [g]**	**β [-]**	**μ [g]**	**β [-]**	**μ [g]**	**β [-]**
89	3	MSN + CR	0.192	0.650	0.328	0.650	0.561	0.650	0.958	0.650	1.638	0.650
90	3	MSN + FLR	0.188	0.675	0.328	0.675	0.573	0.675	1.002	0.675	1.751	0.675
91	≥4	AS-BUILT	0.130	0.625	0.217	0.625	0.363	0.625	0.607	0.625	1.015	0.625
92	≥4	MSN	0.178	0.600	0.292	0.600	0.477	0.600	0.779	0.600	1.274	0.600
93	≥4	CR	0.147	0.650	0.252	0.650	0.430	0.650	0.736	0.650	1.257	0.650
94	≥4	FLR	0.144	0.675	0.252	0.675	0.440	0.675	0.769	0.675	1.344	0.675
95	≥4	MSN + CR	0.181	0.625	0.302	0.625	0.505	0.625	0.843	0.625	1.410	0.625
96	≥4	MSN + FLR	0.177	0.650	0.302	0.650	0.516	0.650	0.882	0.650	1.508	0.650

Table A4. μ (median) and β (standard deviation) values of the as-built and retrofitted fragility models of UniGEa for 1961–1970 masonry buildings.

1961–1970			DS1		DS2		DS3		DS4		DS5	
Id	**N. Storeys**	**Intervention**	**μ [g]**	**β [-]**	**μ [g]**	**β [-]**	**μ [g]**	**β [-]**	**μ [g]**	**β [-]**	**μ [g]**	**β [-]**
97	1	AS-BUILT	0.294	0.600	0.481	0.600	0.786	0.600	1.284	0.600	2.099	0.600
98	1	MSN	0.367	0.600	0.599	0.600	0.979	0.600	1.601	0.600	2.616	0.600
99	1	CR	0.288	0.625	0.481	0.625	0.803	0.625	1.343	0.625	2.244	0.625
100	1	FLR	0.314	0.625	0.525	0.625	0.877	0.625	1.466	0.625	2.451	0.625
101	1	MSN + CR	0.358	0.625	0.599	0.625	1.001	0.625	1.674	0.625	2.798	0.625
102	1	MSN + FLR	0.365	0.625	0.609	0.625	1.019	0.625	1.702	0.625	2.846	0.625
103	2	AS-BUILT	0.285	0.600	0.467	0.600	0.763	0.600	1.247	0.600	2.038	0.600
104	2	MSN	0.356	0.600	0.582	0.600	0.951	0.600	1.554	0.600	2.541	0.600
105	2	CR	0.279	0.625	0.467	0.625	0.780	0.625	1.304	0.625	2.179	0.625
106	2	FLR	0.305	0.625	0.510	0.625	0.852	0.625	1.424	0.625	2.380	0.625
107	2	MSN + CR	0.348	0.625	0.582	0.625	0.972	0.625	1.625	0.625	2.717	0.625
108	2	MSN + FLR	0.354	0.625	0.592	0.625	0.989	0.625	1.653	0.625	2.763	0.625
109	3	AS-BUILT	0.236	0.650	0.403	0.650	0.689	0.650	1.177	0.650	2.012	0.650
110	3	MSN	0.294	0.650	0.502	0.650	0.858	0.650	1.467	0.650	2.508	0.650
111	3	CR	0.252	0.675	0.440	0.675	0.769	0.675	1.344	0.675	2.350	0.675
112	3	FLR	0.252	0.675	0.440	0.675	0.769	0.675	1.344	0.675	2.350	0.675
113	3	MSN + CR	0.292	0.675	0.511	0.675	0.893	0.675	1.561	0.675	2.728	0.675
114	3	MSN + FLR	0.292	0.675	0.511	0.675	0.893	0.675	1.561	0.675	2.728	0.675
115	≥4	AS-BUILT	0.219	0.600	0.358	0.600	0.586	0.600	0.957	0.600	1.564	0.600
116	≥4	MSN	0.273	0.600	0.447	0.600	0.730	0.600	1.193	0.600	1.950	0.600
117	≥4	CR	0.234	0.625	0.391	0.625	0.654	0.625	1.093	0.625	1.827	0.625
118	≥4	FLR	0.229	0.650	0.391	0.650	0.669	0.650	1.143	0.650	1.954	0.650
119	≥4	MSN + CR	0.272	0.625	0.454	0.625	0.759	0.625	1.269	0.625	2.121	0.625
120	≥4	MSN + FLR	0.266	0.650	0.454	0.650	0.776	0.650	1.327	0.650	2.268	0.650

Table A5. μ (median) and β (standard deviation) values of the as-built and retrofitted fragility models of UniGEa for 1971–1980 masonry buildings.

1971–1980			DS1		DS2		DS3		DS4		DS5	
Id	**N. Storeys**	**Intervention**	**μ [g]**	**β [-]**	**μ [g]**	**β [-]**	**μ [g]**	**β [-]**	**μ [g]**	**β [-]**	**μ [g]**	**β [-]**
121	1	AS-BUILT	0.338	0.575	0.541	0.575	0.864	0.575	1.381	0.575	2.208	0.575
122	1	MSN	0.392	0.575	0.626	0.575	1.001	0.575	1.600	0.575	2.557	0.575
123	1	CR	0.331	0.600	0.541	0.600	0.884	0.600	1.444	0.600	2.361	0.600
124	1	FLR	0.341	0.600	0.557	0.600	0.910	0.600	1.487	0.600	2.431	0.600
125	1	MSN + CR	0.383	0.600	0.626	0.600	1.023	0.600	1.673	0.600	2.734	0.600
126	1	MSN + FLR	0.384	0.600	0.628	0.600	1.026	0.600	1.678	0.600	2.742	0.600

Table A5. *Cont.*

1971–1980			DS1		DS2		DS3		DS4		DS5	
Id	**N. Storeys**	**Intervention**	**μ [g]**	**β [-]**	**μ [g]**	**β [-]**	**μ [g]**	**β [-]**	**μ [g]**	**β [-]**	**μ [g]**	**β [-]**
127	2	AS-BUILT	0.321	0.600	0.525	0.600	0.858	0.600	1.402	0.600	2.292	0.600
128	2	MSN	0.372	0.600	0.608	0.600	0.994	0.600	1.624	0.600	2.655	0.600
129	2	CR	0.314	0.625	0.525	0.625	0.877	0.625	1.466	0.625	2.451	0.625
130	2	FLR	0.323	0.625	0.541	0.625	0.904	0.625	1.510	0.625	2.524	0.625
131	2	MSN + CR	0.364	0.625	0.608	0.625	1.016	0.625	1.699	0.625	2.839	0.625
132	2	MSN + FLR	0.365	0.625	0.610	0.625	1.019	0.625	1.704	0.625	2.848	0.625
133	3	AS-BUILT	0.273	0.650	0.467	0.650	0.798	0.650	1.363	0.650	2.330	0.650
134	3	MSN	0.316	0.650	0.541	0.650	0.924	0.650	1.579	0.650	2.699	0.650
135	3	CR	0.267	0.675	0.467	0.675	0.816	0.675	1.426	0.675	2.492	0.675
136	3	FLR	0.275	0.675	0.481	0.675	0.840	0.675	1.468	0.675	2.566	0.675
137	3	MSN + CR	0.309	0.675	0.541	0.675	0.945	0.675	1.651	0.675	2.886	0.675
138	3	MSN + FLR	0.310	0.675	0.542	0.675	0.948	0.675	1.656	0.675	2.895	0.675
139	≥4	AS-BUILT	0.254	0.600	0.415	0.600	0.678	0.600	1.109	0.600	1.812	0.600
140	≥4	MSN	0.294	0.600	0.481	0.600	0.786	0.600	1.284	0.600	2.099	0.600
141	≥4	CR	0.248	0.625	0.415	0.625	0.694	0.625	1.159	0.625	1.938	0.625
142	≥4	FLR	0.256	0.625	0.427	0.625	0.714	0.625	1.194	0.625	1.995	0.625
143	≥4	MSN + CR	0.288	0.625	0.481	0.625	0.803	0.625	1.343	0.625	2.244	0.625
144	≥4	MSN + FLR	0.288	0.625	0.482	0.625	0.806	0.625	1.347	0.625	2.251	0.625

Table A6. μ (median) and β (standard deviation) values of the as-built and retrofitted fragility models of UniPD for pre-1919 masonry buildings (data originally provided in [24]).

Pre-1919			DS1		DS2		DS3		DS4		DS5	
Id	**N. Storeys**	**Intervention**	**μ [g]**	**β [-]**	**μ [g]**	**β [-]**	**μ [g]**	**β [-]**	**μ [g]**	**β [-]**	**μ [g]**	**β [-]**
1, 10	1–2	AS-BUILT	0.098	0.693	0.173	0.715	0.280	0.718	0.453	0.751	0.825	0.793
2, 11	1–2	MSN1	0.132	0.707	0.234	0.732	0.378	0.725	0.611	0.725	1.110	0.716
3, 12	1–2	MSN2	0.154	0.694	0.274	0.726	0.442	0.735	0.715	0.758	1.301	0.684
4, 13	1–2	TR	0.112	0.740	0.198	0.768	0.320	0.755	0.517	0.766	0.948	0.804
5, 14	1–2	FLR	0.126	0.737	0.223	0.760	0.360	0.749	0.582	0.753	1.059	0.758
6, 15	1–2	MSN1 + TR	0.168	0.692	0.298	0.718	0.481	0.737	0.780	0.778	1.425	0.698
7, 16	1–2	MSN1 + FLR	0.205	0.702	0.365	0.703	0.588	0.683	0.945	0.677	1.685	0.670
8, 17	1–2	MSN2 + TR	0.190	0.730	0.338	0.737	0.545	0.729	0.879	0.761	1.579	0.711
9, 18	1–2	MSN2 + FLR	0.264	0.737	0.469	0.738	0.758	0.726	1.223	0.653	2.172	0.611
19, 28	≥3	AS-BUILT	0.073	0.747	0.129	0.776	0.209	0.784	0.337	0.781	0.612	0.808
20, 29	≥3	MSN1	0.111	0.756	0.197	0.786	0.317	0.774	0.514	0.785	0.942	0.816
21, 30	≥3	MSN2	0.127	0.748	0.225	0.780	0.363	0.767	0.587	0.772	1.068	0.767
22, 31	≥3	TR	0.078	0.736	0.139	0.757	0.224	0.761	0.362	0.770	0.656	0.806
23, 32	≥3	FLR	0.091	0.681	0.162	0.702	0.262	0.706	0.424	0.735	0.770	0.774
24, 33	≥3	MSN1 + TR	0.119	0.744	0.212	0.768	0.342	0.756	0.553	0.756	1.009	0.778
25, 34	≥3	MSN1 + FLR	0.148	0.671	0.262	0.694	0.423	0.699	0.684	0.717	1.241	0.672
26, 35	≥3	MSN2 + TR	0.142	0.701	0.253	0.729	0.408	0.733	0.659	0.747	1.196	0.697
27, 36	≥3	MSN2 + FLR	0.184	0.686	0.327	0.700	0.529	0.709	0.856	0.752	1.554	0.708

Table A7. μ (median) and β (standard deviation) values of the as-built and retrofitted fragility models of UniPD for 1919–1945 masonry buildings (data originally provided in [24]).

1919–1945			DS1		DS2		DS3		DS4		DS5	
Id	**N. Storeys**	**Intervention**	**μ [g]**	**β [-]**	**μ [g]**	**β [-]**	**μ [g]**	**β [-]**	**μ [g]**	**β [-]**	**μ [g]**	**β [-]**
37, 46	1–2	AS-BUILT	0.107	0.753	0.190	0.767	0.307	0.765	0.496	0.785	0.910	0.813
38, 47	1–2	MSN1	0.142	0.705	0.253	0.733	0.408	0.742	0.660	0.764	1.197	0.712
39, 48	1–2	MSN2	0.162	0.701	0.287	0.734	0.465	0.754	0.753	0.791	1.373	0.694
40, 49	1–2	TR	0.116	0.771	0.206	0.798	0.332	0.781	0.538	0.774	0.983	0.803

Table A7. *Cont.*

1919–1945			DS1		DS2		DS3		DS4		DS5	
Id	**N. Storeys**	**Intervention**	**μ [g]**	**β [-]**	**μ [g]**	**β [-]**	**μ [g]**	**β [-]**	**μ [g]**	**β [-]**	**μ [g]**	**β [-]**
41, 50	1–2	FLR	0.126	0.741	0.223	0.765	0.360	0.756	0.581	0.762	1.058	0.765
42, 51	1–2	MSN1 + TR	0.173	0.716	0.308	0.743	0.497	0.763	0.807	0.802	1.475	0.705
43, 52	1–2	MSN1 + FLR	0.194	0.697	0.344	0.705	0.555	0.697	0.895	0.727	1.604	0.700
44, 53	1–2	MSN2 + TR	0.191	0.745	0.339	0.755	0.548	0.750	0.884	0.780	1.586	0.711
45, 54	1–2	MSN2 + FLR	0.233	0.696	0.413	0.714	0.665	0.693	1.066	0.627	1.888	0.599
55, 64	≥3	AS-BUILT	0.084	0.719	0.149	0.746	0.241	0.751	0.390	0.768	0.707	0.819
56, 65	≥3	MSN1	0.118	0.784	0.209	0.814	0.338	0.802	0.547	0.802	0.999	0.809
57, 66	≥3	MSN2	0.138	0.728	0.245	0.760	0.395	0.770	0.638	0.790	1.159	0.749
58, 67	≥3	TR	0.088	0.718	0.155	0.739	0.251	0.742	0.405	0.771	0.735	0.819
59, 68	≥3	FLR	0.086	0.725	0.153	0.737	0.247	0.747	0.399	0.768	0.724	0.828
60, 69	≥3	MSN1 + TR	0.123	0.743	0.218	0.775	0.353	0.762	0.570	0.764	1.038	0.773
61, 70	≥3	MSN1 + FLR	0.121	0.701	0.215	0.727	0.347	0.709	0.561	0.708	1.023	0.738
62, 71	≥3	MSN2 + TR	0.146	0.707	0.260	0.733	0.419	0.746	0.678	0.775	1.231	0.709
63, 72	≥3	MSN2 + FLR	0.143	0.687	0.253	0.713	0.409	0.717	0.661	0.732	1.199	0.683

Table A8. μ (median) and β (standard deviation) values of the as-built and retrofitted fragility models of UniPD for 1946–1960 masonry buildings (data originally provided in [24]).

1946–1960			DS1		DS2		DS3		DS4		DS5	
Id	**N. Storeys**	**Intervention**	**μ [g]**	**β [-]**	**μ [g]**	**β [-]**	**μ [g]**	**β [-]**	**μ [g]**	**β [-]**	**μ [g]**	**β [-]**
73, 79	1–2	AS-BUILT	0.150	0.732	0.266	0.760	0.430	0.767	0.696	0.783	1.264	0.704
74, 80	1–2	MSN	0.196	0.750	0.348	0.751	0.561	0.732	0.903	0.747	1.618	0.704
75, 81	1–2	CR	0.170	0.800	0.302	0.818	0.488	0.809	0.792	0.820	1.448	0.702
76, 82	1–2	FLR	0.165	0.774	0.293	0.784	0.474	0.787	0.768	0.807	1.403	0.698
77, 83	1–2	MSN + CR	0.227	0.750	0.403	0.754	0.650	0.728	1.042	0.671	1.846	0.643
78, 84	1–2	MSN + FLR	0.230	0.695	0.409	0.716	0.659	0.696	1.057	0.634	1.871	0.608
85, 91	≥3	AS-BUILT	0.135	0.748	0.240	0.783	0.387	0.782	0.625	0.800	1.134	0.763
86, 92	≥3	MSN	0.189	0.755	0.335	0.761	0.540	0.759	0.873	0.791	1.569	0.714
87, 93	≥3	CR	0.138	0.737	0.244	0.771	0.395	0.775	0.637	0.790	1.157	0.748
88, 94	≥3	FLR	0.133	0.730	0.236	0.764	0.381	0.760	0.616	0.777	1.118	0.753
89, 95	≥3	MSN + CR	0.192	0.759	0.340	0.767	0.549	0.756	0.886	0.778	1.590	0.711
90, 96	≥3	MSN + FLR	0.189	0.689	0.335	0.704	0.541	0.707	0.874	0.753	1.571	0.710

Table A9. μ (median) and β (standard deviation) values of the as-built and retrofitted fragility models of UniPD, for 1961–1980 masonry buildings (data originally provided in [24]).

1961–1980			DS1		DS2		DS3		DS4		DS5	
Id	**N. Storeys**	**Intervention**	**μ [g]**	**β [-]**	**μ [g]**	**β [-]**	**μ [g]**	**β [-]**	**μ [g]**	**β [-]**	**μ [g]**	**β [-]**
97, 103, 121, 127	1–2	AS-BUILT	0.208	0.739	0.369	0.741	0.595	0.716	0.956	0.699	1.703	0.679
98, 104, 122, 128	1–2	MSN	0.267	0.754	0.474	0.760	0.766	0.753	1.237	0.659	2.199	0.608
99, 105, 123, 129	1–2	CR	0.245	0.745	0.435	0.751	0.702	0.731	1.127	0.642	1.995	0.602
100, 106, 124, 130	1–2	FLR	0.233	0.689	0.413	0.707	0.665	0.690	1.066	0.627	1.888	0.599
101, 107, 125, 131	1–2	MSN + CR	0.314	0.791	0.556	0.767	0.895	0.756	1.427	0.681	2.451	0.611
102, 108, 126, 132	1–2	MSN + FLR	0.284	0.696	0.504	0.708	0.816	0.714	1.322	0.662	2.368	0.616
109, 115, 133, 139	≥3	AS-BUILT	0.169	0.676	0.300	0.706	0.485	0.736	0.786	0.785	1.437	0.700
110, 116, 134, 140	≥3	MSN	0.200	0.691	0.354	0.694	0.571	0.680	0.919	0.691	1.644	0.683
111, 117, 135, 141	≥3	CR	0.170	0.688	0.301	0.711	0.487	0.724	0.790	0.760	1.444	0.699
112, 118, 136, 142	≥3	FLR	0.159	0.659	0.283	0.687	0.457	0.702	0.740	0.730	1.348	0.685
113, 119, 137, 143	≥3	MSN + CR	0.207	0.678	0.368	0.689	0.593	0.685	0.953	0.683	1.698	0.671
114, 120, 138, 144	≥3	MSN + FLR	0.196	0.646	0.349	0.657	0.562	0.655	0.906	0.681	1.621	0.682

Table A10. μ (median) and β (standard deviation) values of the as-built and retrofitted fragility models of UniGEb for pre-1919 masonry buildings.

Pre-1919			DS1		DS2		DS3		DS4		DS5	
Id	**N. Storeys**	**Intervention**	**μ [g]**	**β [-]**	**μ [g]**	**β [-]**	**μ [g]**	**β [-]**	**μ [g]**	**β [-]**	**μ [g]**	**β [-]**
1	1	AS-BUILT	0.118	0.714	0.189	0.716	0.304	0.557	0.413	0.531	0.690	0.539
2	1	MSN1	0.185	0.712	0.296	0.715	0.435	0.576	0.523	0.541	0.874	0.548
3	1	MSN2	0.239	0.711	0.384	0.714	0.560	0.582	0.607	0.571	1.015	0.577
4	1	TR	0.149	0.689	0.245	0.689	0.380	0.537	0.489	0.518	0.816	0.525
5	1	FLR	0.165	0.688	0.256	0.688	0.418	0.540	0.511	0.522	0.854	0.528
6	1	MSN1 + TR	0.233	0.691	0.384	0.691	0.576	0.553	0.597	0.546	0.997	0.554
7	1	MSN1 + FLR	0.258	0.690	0.401	0.690	0.640	0.557	0.678	0.553	1.133	0.559
8	1	MSN2 + TR	0.302	0.693	0.497	0.693	0.746	0.562	0.783	0.562	1.309	0.566
9	1	MSN2 + FLR	0.334	0.692	0.519	0.692	0.829	0.568	0.870	0.568	1.454	0.571
10	2	AS-BUILT	0.101	0.665	0.187	0.663	0.274	0.539	0.379	0.525	0.634	0.533
11	2	MSN1	0.150	0.669	0.277	0.668	0.381	0.530	0.512	0.512	0.855	0.518
12	2	MSN2	0.188	0.673	0.348	0.672	0.444	0.543	0.562	0.518	0.939	0.523
13	2	TR	0.128	0.640	0.236	0.639	0.367	0.502	0.479	0.496	0.800	0.502
14	2	FLR	0.143	0.638	0.263	0.637	0.370	0.506	0.475	0.494	0.794	0.499
15	2	MSN1 + TR	0.189	0.648	0.349	0.648	0.464	0.515	0.564	0.504	0.942	0.508
16	2	MSN1 + FLR	0.211	0.646	0.388	0.646	0.511	0.521	0.563	0.510	0.941	0.515
17	2	MSN2 + TR	0.238	0.655	0.439	0.654	0.579	0.523	0.621	0.516	1.037	0.520
18	2	MSN2 + FLR	0.265	0.653	0.488	0.653	0.644	0.528	0.677	0.527	1.131	0.531
19	3	AS-BUILT	0.082	0.628	0.154	0.619	0.288	0.534	0.405	0.527	0.676	0.535
20	3	MSN1	0.119	0.651	0.219	0.650	0.391	0.512	0.542	0.507	0.905	0.512
21	3	MSN2	0.147	0.656	0.272	0.655	0.428	0.511	0.592	0.506	0.988	0.510
22	3	TR	0.104	0.619	0.192	0.618	0.381	0.497	0.505	0.497	0.843	0.502
23	3	FLR	0.116	0.619	0.214	0.619	0.387	0.493	0.511	0.493	0.854	0.498
24	3	MSN1 + TR	0.150	0.631	0.277	0.630	0.445	0.495	0.587	0.495	0.981	0.499
25	3	MSN1 + FLR	0.167	0.628	0.309	0.628	0.453	0.494	0.595	0.493	0.993	0.497
26	3	MSN2 + TR	0.186	0.638	0.344	0.637	0.487	0.497	0.641	0.497	1.071	0.500
27	3	MSN2 + FLR	0.207	0.635	0.383	0.635	0.507	0.500	0.649	0.498	1.084	0.501
28	≥4	AS-BUILT	0.072	0.573	0.162	0.533	0.241	0.580	0.349	0.564	0.582	0.573
29	≥4	MSN1	0.102	0.620	0.189	0.616	0.358	0.535	0.503	0.526	0.841	0.532
30	≥4	MSN2	0.125	0.638	0.230	0.637	0.391	0.531	0.548	0.521	0.915	0.527
31	≥4	TR	0.090	0.574	0.174	0.559	0.405	0.499	0.539	0.499	0.901	0.504
32	≥4	FLR	0.101	0.588	0.187	0.583	0.410	0.496	0.543	0.496	0.908	0.501
33	≥4	MSN1 + TR	0.128	0.615	0.237	0.614	0.471	0.496	0.624	0.496	1.042	0.500
34	≥4	MSN1 + FLR	0.143	0.615	0.264	0.615	0.476	0.492	0.629	0.492	1.050	0.496
35	≥4	MSN2 + TR	0.158	0.625	0.291	0.624	0.513	0.494	0.679	0.494	1.134	0.497
36	≥4	MSN2 + FLR	0.176	0.622	0.324	0.622	0.518	0.492	0.684	0.492	1.142	0.495

Table A11. μ (median) and β (standard deviation) values of the as-built and retrofitted fragility models of UniGEb for 1919–1945 masonry buildings.

1919–1945			DS1		DS2		DS3		DS4		DS5	
Id	**N. Storeys**	**Intervention**	**μ [g]**	**β [-]**	**μ [g]**	**β [-]**	**μ [g]**	**β [-]**	**μ [g]**	**β [-]**	**μ [g]**	**β [-]**
37	1	AS-BUILT	0.136	0.775	0.218	0.777	0.344	0.615	0.451	0.568	0.764	0.582
38	1	MSN1	0.206	0.769	0.331	0.771	0.488	0.637	0.576	0.593	0.976	0.607
39	1	MSN2	0.256	0.758	0.411	0.759	0.602	0.629	0.654	0.610	1.108	0.622
40	1	TR	0.169	0.740	0.277	0.738	0.425	0.589	0.525	0.553	0.889	0.566
41	1	FLR	0.186	0.736	0.289	0.736	0.466	0.590	0.552	0.560	0.935	0.573
42	1	MSN1 + TR	0.256	0.739	0.422	0.738	0.634	0.601	0.659	0.598	1.117	0.614
43	1	MSN1 + FLR	0.283	0.736	0.439	0.736	0.700	0.602	0.740	0.598	1.255	0.612
44	1	MSN2 + TR	0.318	0.732	0.523	0.731	0.788	0.598	0.829	0.596	1.406	0.606
45	1	MSN2 + FLR	0.351	0.730	0.544	0.730	0.870	0.602	0.914	0.601	1.549	0.610

Table A11. *Cont.*

1919–1945			DS1		DS2		DS3		DS4		DS5	
Id	**N. Storeys**	**Intervention**	**μ [g]**	**β [-]**	**μ [g]**	**β [-]**	**μ [g]**	**β [-]**	**μ [g]**	**β [-]**	**μ [g]**	**β [-]**
46	2	AS-BUILT	0.116	0.717	0.213	0.712	0.307	0.568	0.417	0.545	0.707	0.560
47	2	MSN1	0.168	0.720	0.308	0.715	0.422	0.570	0.556	0.540	0.943	0.553
48	2	MSN2	0.203	0.714	0.373	0.710	0.482	0.574	0.605	0.544	1.025	0.555
49	2	TR	0.144	0.683	0.265	0.680	0.394	0.526	0.503	0.513	0.853	0.523
50	2	FLR	0.159	0.679	0.292	0.677	0.402	0.538	0.497	0.514	0.843	0.523
51	2	MSN1 + TR	0.208	0.690	0.382	0.688	0.510	0.553	0.603	0.534	1.023	0.545
52	2	MSN1 + FLR	0.229	0.687	0.421	0.685	0.557	0.556	0.605	0.543	1.025	0.555
53	2	MSN2 + TR	0.252	0.689	0.463	0.687	0.615	0.551	0.657	0.541	1.115	0.551
54	2	MSN2 + FLR	0.278	0.686	0.510	0.685	0.676	0.555	0.714	0.551	1.210	0.560
55	3	AS-BUILT	0.094	0.683	0.174	0.673	0.317	0.547	0.445	0.541	0.755	0.555
56	3	MSN1	0.133	0.699	0.244	0.694	0.423	0.530	0.584	0.525	0.989	0.536
57	3	MSN2	0.159	0.694	0.292	0.690	0.458	0.528	0.628	0.521	1.065	0.530
58	3	TR	0.117	0.660	0.215	0.657	0.398	0.508	0.530	0.508	0.898	0.517
59	3	FLR	0.129	0.657	0.236	0.655	0.403	0.505	0.534	0.506	0.906	0.515
60	3	MSN1 + TR	0.165	0.670	0.303	0.667	0.474	0.516	0.623	0.515	1.057	0.525
61	3	MSN1 + FLR	0.182	0.666	0.334	0.664	0.480	0.516	0.628	0.515	1.065	0.525
62	3	MSN2 + TR	0.198	0.669	0.363	0.667	0.513	0.516	0.671	0.515	1.137	0.523
63	3	MSN2 + FLR	0.218	0.666	0.400	0.665	0.533	0.518	0.676	0.516	1.146	0.524
64	≥4	AS-BUILT	0.082	0.630	0.174	0.579	0.270	0.594	0.390	0.580	0.661	0.597
65	≥4	MSN1	0.113	0.669	0.209	0.662	0.386	0.548	0.543	0.540	0.920	0.553
66	≥4	MSN2	0.135	0.674	0.248	0.670	0.416	0.541	0.583	0.533	0.989	0.544
67	≥4	TR	0.101	0.617	0.190	0.604	0.422	0.508	0.565	0.508	0.957	0.516
68	≥4	FLR	0.112	0.626	0.206	0.622	0.426	0.506	0.567	0.505	0.961	0.514
69	≥4	MSN1 + TR	0.141	0.653	0.259	0.650	0.497	0.513	0.661	0.513	1.121	0.523
70	≥4	MSN1 + FLR	0.155	0.651	0.285	0.649	0.501	0.510	0.663	0.511	1.125	0.520
71	≥4	MSN2 + TR	0.168	0.654	0.307	0.652	0.535	0.509	0.709	0.509	1.203	0.517
72	≥4	MSN2 + FLR	0.184	0.652	0.338	0.651	0.538	0.507	0.712	0.507	1.207	0.515

Table A12. μ (median) and β (standard deviation) values of the as-built and retrofitted fragility models of UniGEb for 1946–1960 masonry buildings.

1946–1960			DS1		DS2		DS3		DS4		DS5	
Id	**N. Storeys**	**Intervention**	**μ [g]**	**β [-]**	**μ [g]**	**β [-]**	**μ [g]**	**β [-]**	**μ [g]**	**β [-]**	**μ [g]**	**β [-]**
73	1	AS-BUILT	0.174	0.854	0.280	0.853	0.436	0.692	0.531	0.628	0.877	0.628
74	1	MSN	0.306	0.820	0.490	0.820	0.731	0.689	0.781	0.673	1.288	0.673
75	1	CR	0.204	0.811	0.332	0.807	0.511	0.655	0.595	0.608	0.982	0.608
76	1	FLR	0.221	0.803	0.344	0.803	0.553	0.650	0.627	0.614	1.035	0.614
77	1	MSN + CR	0.357	0.788	0.583	0.785	0.887	0.645	0.933	0.643	1.539	0.643
78	1	MSN + FLR	0.387	0.782	0.602	0.782	0.964	0.643	1.013	0.643	1.671	0.643
79	2	AS-BUILT	0.144	0.783	0.260	0.770	0.368	0.599	0.475	0.564	0.783	0.564
80	2	MSN	0.237	0.768	0.426	0.757	0.570	0.620	0.689	0.581	1.137	0.581
81	2	CR	0.168	0.742	0.303	0.734	0.435	0.560	0.529	0.540	0.873	0.540
82	2	FLR	0.183	0.734	0.329	0.728	0.449	0.574	0.525	0.544	0.866	0.544
83	2	MSN + CR	0.276	0.737	0.497	0.731	0.678	0.586	0.724	0.579	1.194	0.579
84	2	MSN + FLR	0.300	0.732	0.540	0.729	0.734	0.587	0.773	0.584	1.275	0.584
85	3	AS-BUILT	0.115	0.746	0.209	0.729	0.359	0.553	0.502	0.548	0.828	0.548
86	3	MSN	0.184	0.743	0.331	0.732	0.513	0.546	0.683	0.538	1.127	0.538
87	3	CR	0.135	0.713	0.242	0.705	0.412	0.526	0.553	0.525	0.913	0.525
88	3	FLR	0.146	0.706	0.263	0.701	0.416	0.526	0.557	0.524	0.919	0.524
89	3	MSN + CR	0.215	0.713	0.386	0.708	0.551	0.539	0.708	0.537	1.169	0.537
90	3	MSN + FLR	0.233	0.708	0.419	0.705	0.565	0.540	0.713	0.540	1.176	0.540

Table A12. *Cont.*

1946–1960			DS1		DS2		DS3		DS4		DS5	
Id	**N. Storeys**	**Intervention**	**μ [g]**	**β [-]**	**μ [g]**	**β [-]**	**μ [g]**	**β [-]**	**μ [g]**	**β [-]**	**μ [g]**	**β [-]**
91	≥4	AS-BUILT	0.099	0.692	0.196	0.634	0.320	0.593	0.456	0.582	0.753	0.582
92	≥4	MSN	0.155	0.721	0.279	0.710	0.465	0.551	0.648	0.544	1.069	0.544
93	≥4	CR	0.116	0.666	0.211	0.649	0.431	0.525	0.582	0.522	0.961	0.522
94	≥4	FLR	0.126	0.668	0.227	0.661	0.433	0.523	0.584	0.520	0.963	0.520
95	≥4	MSN + CR	0.181	0.695	0.325	0.690	0.558	0.528	0.746	0.527	1.231	0.527
96	≥4	MSN + FLR	0.196	0.690	0.352	0.688	0.560	0.527	0.748	0.526	1.233	0.526

Table A13. μ (median) and β (standard deviation) values of the as-built and retrofitted fragility models of UniGEb for 1961–1980 masonry buildings.

1961–1980			DS1		DS2		DS3		DS4		DS5	
Id	**N. Storeys**	**Intervention**	**μ [g]**	**β [-]**	**μ [g]**	**β [-]**	**μ [g]**	**β [-]**	**μ [g]**	**β [-]**	**μ [g]**	**β [-]**
97, 121	1	AS-BUILT	0.271	0.805	0.432	0.802	0.676	0.673	0.740	0.632	1.198	0.649
98, 122	1	MSN	0.394	0.773	0.627	0.771	0.971	0.654	1.021	0.649	1.655	0.663
99, 123	1	CR	0.291	0.772	0.468	0.767	0.733	0.636	0.793	0.607	1.284	0.624
100, 124	1	FLR	0.306	0.763	0.477	0.763	0.771	0.626	0.828	0.605	1.341	0.622
101, 125	1	MSN + CR	0.423	0.749	0.679	0.745	1.063	0.615	1.117	0.615	1.810	0.627
102, 126	1	MSN + FLR	0.445	0.742	0.693	0.742	1.119	0.609	1.175	0.609	1.905	0.620
103, 127	2	AS-BUILT	0.208	0.742	0.358	0.724	0.504	0.599	0.586	0.560	0.949	0.574
104, 128	2	MSN	0.290	0.728	0.499	0.713	0.714	0.600	0.813	0.566	1.317	0.578
105, 129	2	CR	0.223	0.712	0.384	0.700	0.548	0.564	0.610	0.545	0.988	0.556
106, 130	2	FLR	0.235	0.702	0.404	0.696	0.569	0.568	0.608	0.549	0.986	0.560
107, 131	2	MSN + CR	0.311	0.705	0.535	0.698	0.777	0.567	0.833	0.561	1.350	0.572
108, 132	2	MSN + FLR	0.327	0.699	0.563	0.696	0.816	0.561	0.853	0.561	1.382	0.571
109, 133	3	AS-BUILT	0.159	0.708	0.273	0.689	0.430	0.544	0.566	0.528	0.916	0.540
110, 134	3	MSN	0.216	0.705	0.372	0.690	0.582	0.528	0.729	0.523	1.181	0.532
111, 135	3	CR	0.170	0.681	0.293	0.670	0.453	0.528	0.586	0.518	0.949	0.526
112, 136	3	FLR	0.179	0.672	0.308	0.667	0.456	0.528	0.587	0.518	0.952	0.526
113, 137	3	MSN + CR	0.232	0.683	0.399	0.676	0.603	0.522	0.742	0.523	1.203	0.531
114, 138	3	MSN + FLR	0.244	0.677	0.420	0.675	0.608	0.522	0.745	0.524	1.206	0.532
115, 139	≥4	AS-BUILT	0.133	0.668	0.235	0.628	0.397	0.557	0.541	0.543	0.876	0.558
116, 140	≥4	MSN	0.178	0.686	0.307	0.672	0.536	0.531	0.713	0.523	1.155	0.533
117, 141	≥4	CR	0.142	0.644	0.246	0.628	0.452	0.526	0.600	0.520	0.972	0.527
118, 142	≥4	FLR	0.150	0.638	0.258	0.632	0.453	0.525	0.600	0.519	0.973	0.526
119, 143	≥4	MSN + CR	0.191	0.667	0.329	0.660	0.591	0.518	0.770	0.517	1.248	0.525
120, 144	≥4	MSN + FLR	0.201	0.661	0.346	0.660	0.592	0.518	0.770	0.517	1.248	0.524

References

1. Italian Civil Protection Department National Risk Assessment. *Overview of the Potential Major Disasters in Italy: Seismic, Volcanic, Tsunami, Hydrogeological/Hydraulic and Extreme Weather, Droughts and Forest Fire Risks 2018*; Italian Civil Protection Department National Risk Assessment: Rome, Italy, 2018.
2. Augenti, N.; Parisi, F. Learning from Construction Failures Due to the 2009 L'Aquila, Italy, Earthquake. *J. Perform. Constr. Facil.* **2010**, *24*, 536–555. [CrossRef]
3. Sorrentino, L.; Cattari, S.; da Porto, F.; Magenes, G.; Penna, A. Seismic Behaviour of Ordinary Masonry Buildings during the 2016 Central Italy Earthquakes. *Bull. Earthq. Eng.* **2019**, *17*, 5583–5607. [CrossRef]
4. Valluzzi, M.R.; Sbrogiò, L.; Saretta, Y.; Wenliuhan, H. Seismic Response of Masonry Buildings in Historical Centres Struck by the 2016 Central Italy Earthquake. Impact of Building Features on Damage Evaluation. *Int. J. Archit. Herit.* **2021**, *16*, 1859–1884. [CrossRef]
5. Dolce, M.; Prota, A.; Borzi, B.; da Porto, F.; Lagomarsino, S.; Magenes, G.; Moroni, C.; Penna, A.; Polese, M.; Speranza, E.; et al. Seismic Risk Assessment of Residential Buildings in Italy. *Bull. Earthq. Eng.* **2021**, *19*, 2999–3032. [CrossRef]
6. Masi, A.; Lagomarsino, S.; Dolce, M.; Manfredi, V.; Ottonelli, D. Towards the Updated Italian Seismic Risk Assessment: Exposure and Vulnerability Modelling. *Bull. Earthq. Eng.* **2021**, *19*, 3253–3286. [CrossRef]

7. Lagomarsino, S. *The MARS Vulnerability Model: A New Metrics Based on EMS-98 Vulnerability Classes*; Conspress: Bucharest, Romania, 2022; pp. 3327–3336.
8. Cattari, S.; Alfano, S.; Masi, A.; Manfredi, V.; Borzi, B.; Di Meo, A.; da Porto, F.; Saler, E.; Dall'Asta, A.; Gioiella, L.; et al. *Risk Assessment of Italian School Buildings at National Scale: The MARS Project Experience*; Conspress: Bucharest, Romania, 2022; pp. 3383–3392.
9. Di Meo, A.; Faravelli, M.; Pascale, V.; Borzi, B.; Calderini, C.; Sisti, R.; Speranza, E.; Bocchi, F. Damage Survey on Churches: A New Observed Damage Database of Past Italian Earthquakes (Da.D.O.). *Int. J. Disaster Risk Reduct.* **2023**, *87*, 103595. [CrossRef]
10. Calvi, G.M.; Pinho, R.; Magenes, G.; Bommer, J.J.; Restrepo-Vélez, L.F.; Crowley, H. Development of Seismic Vulnerability Assessment Methodologies over the Past 30 Years. *ISET J. Earthq. Technol.* **2006**, *43*, 75–104.
11. ISTAT 15° Censimento della Popolazione e delle Abitazioni 2011. Website and Data Warehouse. Available online: https://www.istat.it/it/censimenti-permanenti/censimenti-precedenti/popolazione-e-abitazioni/popolazione-2011 (accessed on 26 September 2022).
12. Borzi, B.; Faravelli, M.; Di Meo, A. Application of the SP-BELA Methodology to RC Residential Buildings in Italy to Produce Seismic Risk Maps for the National Risk Assessment. *Bull. Earthq. Eng.* **2021**, *19*, 3185–3208. [CrossRef]
13. Donà, M.; Carpanese, P.; Follador, V.; Sbrogiò, L.; da Porto, F. Mechanics-Based Fragility Curves for Italian Residential URM Buildings. *Bull. Earthq. Eng.* **2021**, *19*, 3099–3127. [CrossRef]
14. Rosti, A.; Del Gaudio, C.; Rota, M.; Ricci, P.; Di Ludovico, M.; Penna, A.; Verderame, G.M. Empirical Fragility Curves for Italian Residential RC Buildings. *Bull. Earthq. Eng.* **2021**, *19*, 3165–3183. [CrossRef]
15. Rosti, A.; Rota, M.; Penna, A. Empirical Fragility Curves for Italian URM Buildings. *Bull. Earthq. Eng.* **2021**, *19*, 3057–3076. [CrossRef]
16. Zuccaro, G.; Perelli, F.L.; De Gregorio, D.; Cacace, F. Empirical Vulnerability Curves for Italian Mansory Buildings: Evolution of Vulnerability Model from the DPM to Curves as a Function of Accelertion. *Bull. Earthq. Eng.* **2021**, *19*, 3077–3097. [CrossRef]
17. Lagomarsino, S.; Cattari, S.; Ottonelli, D. The Heuristic Vulnerability Model: Fragility Curves for Masonry Buildings. *Bull. Earthq. Eng.* **2021**, *19*, 3129–3163. [CrossRef]
18. Cao, X.-Y. An Iterative PSD-Based Procedure for the Gaussian Stochastic Earthquake Model with Combined Intensity and Frequency Nonstationarities: Its Application into Precast Concrete Structures. *Mathematics* **2023**, *11*, 1294. [CrossRef]
19. Smerzini, C.; Galasso, C.; Iervolino, I.; Paolucci, R. Ground Motion Record Selection Based on Broadband Spectral Compatibility. *Earthq. Spectra* **2014**, *30*, 1427–1448. [CrossRef]
20. Manfredi, V.; Masi, A.; Özcebe, A.G.; Paolucci, R.; Smerzini, C. Selection and Spectral Matching of Recorded Ground Motions for Seismic Fragility Analyses. *Bull. Earthq. Eng.* **2022**, *20*, 4961–4987. [CrossRef]
21. Feng, D.-C.; Cao, X.-Y.; Beer, M. An Enhanced PDEM-Based Framework for Reliability Analysis of Structures Considering Multiple Failure Modes and Limit States. *Probabilistic Eng. Mech.* **2022**, *70*, 103367. [CrossRef]
22. Cattari, S.; Angiolilli, M. Multiscale Procedure to Assign Structural Damage Levels in Masonry Buildings from Observed or Numerically Simulated Seismic Performance. *Bull. Earthq. Eng.* **2022**, *20*, 7561–7607. [CrossRef]
23. da Porto, F.; Lagomarsino, S.; Cattari, S.; Follador, V.; Carpanese, P.; Donà, M.; Alfano, S. *Fragility Curves of As-Built and Retrofitted Masonry Buildings in Italy*; Conspress: Bucharest, Romania, 2022; pp. 3337–3346.
24. Follador, V.; Carpanese, P.; Donà, M.; da Porto, F. Effect of Retrofit Interventions on Seismic Fragility of Italian Residential Masonry Buildings. *Int. J. Disaster Risk Reduct.* **2023**, *91*, 103668. [CrossRef]
25. Gentile, R.; Galasso, C. Simplified Seismic Loss Assessment for Optimal Structural Retrofit of RC Buildings. *Earthq. Spectra* **2021**, *37*, 346–365. [CrossRef]
26. Aljawhari, K.; Gentile, R.; Galasso, C. A Fragility-Oriented Approach for Seismic Retrofit Design. *Earthq. Spectra* **2022**, *38*, 1813–1843. [CrossRef]
27. Xu, J.-G.; Cao, X.-Y.; Wu, G. Seismic Collapse and Reparability Performance of Reinforced Concrete Frames Retrofitted with External PBSPC BRBF Sub-Frame in near-Fault Regions. *J. Build. Eng.* **2023**, *64*, 105716. [CrossRef]
28. Sbrogiò, L.; Saretta, Y.; Valluzzi, M.R. Empirical Performance Levels of Strengthened Masonry Buildings Struck by the 2016 Central Italy Earthquake: Proposal of a New Taxonomy. *Int. J. Archit. Herit.* **2023**, *17*, 1017–1042. [CrossRef]
29. Vettore, M.; Saretta, Y.; Sbrogiò, L.; Valluzzi, M.R. A New Methodology for the Survey and Evaluation of Seismic Damage and Vulnerability Entailed by Structural Interventions on Masonry Buildings: Validation on the Town of Castelsantangelo Sul Nera (MC), Italy. *Int. J. Archit. Herit.* **2022**, *16*, 182–207. [CrossRef]
30. Da Porto, F.; Valluzzi, M.R.; Munari, M.; Modena, C.; Arêde, A.; Costa, A.A. Strengthening of Stone and Brick Masonry Buildings. In *Strengthening and Retrofitting of Existing Structures*; Costa, A., Arêde, A., Varum, H., Eds.; Building Pathology and Rehabilitation; Springer: Singapore, 2018; Volume 9, pp. 59–84. ISBN 978-981-10-5857-8.
31. Saretta, Y.; Sbrogiò, L.; Valluzzi, M.R. Seismic Response of Masonry Buildings in Historical Centres Struck by the 2016 Central Italy Earthquake. Calibration of a Vulnerability Model for Strengthened Conditions. *Constr. Build. Mater.* **2021**, *299*, 123911. [CrossRef]
32. Oliveira, D.V.; Silva, R.A.; Garbin, E.; Lourenço, P.B. Strengthening of Three-Leaf Stone Masonry Walls: An Experimental Research. *Mater. Struct.* **2012**, *45*, 1259–1276. [CrossRef]
33. Silva, B.; Dalla Benetta, M.; da Porto, F.; Valluzzi, M.R. Compression and Sonic Tests to Assess Effectiveness of Grout Injection on Three-Leaf Stone Masonry Walls. *Int. J. Archit. Herit.* **2014**, *8*, 408–435. [CrossRef]

34. de Felice, G.; De Santis, S.; Garmendia, L.; Ghiassi, B.; Larrinaga, P.; Lourenço, P.B.; Oliveira, D.V.; Paolacci, F.; Papanicolaou, C.G. Mortar-Based Systems for Externally Bonded Strengthening of Masonry. *Mater. Struct.* **2014**, *47*, 2021–2037. [CrossRef]
35. Giaretton, M.; Dizhur, D.; Garbin, E.; Ingham, J.; da Porto, F. In-Plane Strengthening of Clay Brick and Block Masonry Walls Using Textile-Reinforced Mortar. *J. Compos. Constr.* **2018**, *22*, 04018028. [CrossRef]
36. Valluzzi, M.; Sbrogiò, L.; Saretta, Y. Intervention Strategies for the Seismic Improvement of Masonry Buildings Based on FME Validation: The Case of a Terraced Building Struck by the 2016 Central Italy Earthquake. *Buildings* **2021**, *11*, 404. [CrossRef]
37. Modena, C.; Valluzzi, M.R.; da Porto, F.; Casarin, F. Structural Aspects of The Conservation of Historic Masonry Constructions in Seismic Areas: Remedial Measures and Emergency Actions. *Int. J. Archit. Herit.* **2011**, *5*, 539–558. [CrossRef]
38. Calderini, C.; Piccardo, P.; Vecchiattini, R. Experimental Characterization of Ancient Metal Tie-Rods in Historic Masonry Buildings. *Int. J. Archit. Herit.* **2019**, *13*, 425–437. [CrossRef]
39. Podestà, S.; Scandolo, L. Earthquakes and Tie-Rods: Assessment, Design, and Ductility Issues. *Int. J. Archit. Herit.* **2019**, *13*, 329–339. [CrossRef]
40. Graziotti, F.; Tomassetti, U.; Penna, A.; Magenes, G. Out-of-Plane Shaking Table Tests on URM Single Leaf and Cavity Walls. *Eng. Struct.* **2016**, *125*, 455–470. [CrossRef]
41. *CNR-DT 212/2013*; Istruzioni per la Valutazione Affidabilistica della Sicurezza Sismica di Edifici Esistenti. CNR: Rome, Italy, 2014.
42. Magenes, G.; Penna, A.; Senaldi, I.E.; Rota, M.; Galasco, A. Shaking Table Test of a Strengthened Full-Scale Stone Masonry Building with Flexible Diaphragms. *Int. J. Archit. Herit.* **2014**, *8*, 349–375. [CrossRef]
43. Senaldi, I.; Magenes, G.; Penna, A.; Galasco, A.; Rota, M. The Effect of Stiffened Floor and Roof Diaphragms on the Experimental Seismic Response of a Full-Scale Unreinforced Stone Masonry Building. *J. Earthq. Eng.* **2014**, *18*, 407–443. [CrossRef]
44. Lagomarsino, S.; Giovinazzi, S. Macroseismic and Mechanical Models for the Vulnerability and Damage Assessment of Current Buildings. *Bull. Earthq. Eng.* **2006**, *4*, 415–443. [CrossRef]
45. Grünthal, G. (Ed.) *European Macroseismic Scale 1998: EMS-98*; Cahiers du Centre Européen de Géodynamique et de Séismologie; European Seismological Commission, Subcommission on Engineering Seismology; Working Group Macroseismic Scales: Luxembourg, 1998; Volume 15, ISBN 978-2-87977-008-6.
46. Di Ludovico, M.; Cattari, S.; Verderame, G.; Del Vecchio, C.; Ottonelli, D.; Del Gaudio, C.; Prota, A.; Lagomarsino, S. Fragility Curves of Italian School Buildings: Derivation from L'Aquila 2009 Earthquake Damage via Observational and Heuristic Approaches. *Bull. Earthq. Eng.* **2023**, *21*, 397–432. [CrossRef]
47. Bernardini, A.; Gori, M.; Modena, C. Application of Coupled Analytical Models and Experimental Knowledge to Seismic Vulnerability Analyses of Masonry Buildings. In *Earthquake Damage Evaluation and Vulnerability Analysis of Building Structures*; Omega Scientific: Oxford, UK, 1990; Volume 3, pp. 161–180.
48. Valluzzi, M.R.; Follador, V.; Sbrogiò, L. Vulnus Web: A Web-Based Procedure for the Seismic Vulnerability Assessment of Masonry Buildings. *Sustainability* **2023**, *15*, 6787. [CrossRef]
49. Ferrini, M.; Melozzi, A.; Pagliazzi, A.; Scarparolo, S. Rilevamento della Vulnerabilità Sismica Degli Edifici in Muratura. Manuale per la Compilazione della Scheda GNDT/CNR di II Livello. Regione Toscana, Italy. 2003. Available online: https://www.abacomurature.it/pdf/01%20Manuale%20compilazione%20schede%20II%20liv_GNDT.pdf (accessed on 16 August 2023).
50. Lagomarsino, S.; Cattari, S. Fragility Functions of Masonry Buildings. In *SYNER-G: Typology Definition and Fragility Functions for Physical Elements at Seismic Risk*; Pitilakis, K., Crowley, H., Kaynia, A.M., Eds.; Geotechnical, Geological and Earthquake Engineering; Springer: Dordrecht, The Netherlands, 2014; Volume 27, pp. 111–156. ISBN 978-94-007-7871-9.
51. Cattari, S.; Alfano, S.; Ottonelli, D.; Saler, E.; Da Porto, F. Comparative Study on Two Analytical Mechanical-Based Methods for Deriving Fragility Curves Targeted to Masonry School Buildings. In Proceedings of the 8th International Conference on Computational Methods in Structural Dynamics and Earthquake Engineering Methods in Structural Dynamics and Earthquake Engineering, Athens, Greece, 28–30 June 2021; pp. 3155–3175.
52. Freeman, S.A. The Capacity Spectrum Method as a Tool for Seismic Design. In Proceedings of the 11th European Conference on Earthquake Engineering, Paris, France, 6–11 September 1998.
53. da Porto, F.; Donà, M.; Rosti, A.; Rota, M.; Lagomarsino, S.; Cattari, S.; Borzi, B.; Onida, M.; De Gregorio, D.; Perelli, F.L.; et al. Comparative Analysis of the Fragility Curves for Italian Residential Masonry and RC Buildings. *Bull. Earthq. Eng.* **2021**, *19*, 3209–3252. [CrossRef]
54. Dolce, M.; Speranza, E.; Giordano, F.; Borzi, B.; Bocchi, F.; Conte, C.; Di Meo, A.; Faravelli, M.; Pascale, V. Observed Damage Database of Past Italian Earthquakes: The Da.D.O. WebGIS. *Boll. Geofis. Teor. Appl.* **2019**, *60*, 141–164.